Monatshefte für Chemie 136, 289–324 (2005)
DOI 10.1007/s00706-005-0282-2

Monatshefte für Chemie
Chemical Monthly
Printed in Austria

Exciton Chirality Method. Oriented Molecules – Anisotropic Phases

Hans-Georg Kuball[1,*], **Elmar Dorr**[2], **Tatjana Höfer**[3], and **Oliver Türk**[4]

[1] Department of Chemistry – Physical Chemistry, University of Kaiserslautern, Postfach 3049, D-67653 Kaiserslautern, Germany
[2] D-76870 Kandel, Germany
[3] D-64390 Erzhausen, Germany
[4] Lonza Compounds GmbH & Co. KG, D-56357 Miehlen, Germany

Received November 12, 2004; accepted (revised) December 20, 2004
Published online March 8, 2005

Summary. The results of the theory of the anisotropy of optical activity (ACD), especially of the circular dichroism (CD), in view of its application to the exciton chirality method was presented. In order to introduce the phenomenology some typical experimental anisotropy effects of the ACD of a dibenzoate and two taddoles were discussed. The CD and ACD of unbridged and bridged 1,1′-binaphthols were described taking into account results of the polarized spectroscopy. Their CD and ACD spectra were decomposed into contributions of their two exciton transitions. It was proven that the electric dipole/electric quadrupole transition moments contribute in same order of magnitude as the electric dipole/magnetic dipole transition moments to the tensor coordinates of the CD tensor for a bridged 1,1′-binaphthol. The CD tensor coordinates $\Delta\varepsilon_{ii}^{*}$ for a light beam propagation along the principal axes of the order tensor of a 1,1′-binaphthol of approximately C_2 symmetry are very different in size and also of different sign. The largest tensor coordinate belongs to the direction along the naphthyl–naphthyl bond. The CD along the C_2 symmetry axis is approximately zero. The CD tensor coordinates of different sign along different directions within a molecule can be assigned to different helicities in their molecular structure along these directions. For (*R*)-1,1′-binaphthol skeleton the left handed helix along an axis, which is perpendicular to the naphthyl–naphthyl bond and perpendicular to the C_2 symmetry axis, leads to a positive couplet whereas for the right-handed helix along the naphthyl–naphthyl bond a negative couplet has been found. Thus, the ACD with its determination of the $\Delta\varepsilon_{ii}^{*}$ allows to observe different helicities along different directions within a molecule. As well for the bridged as the unbridged binaphthols in the spectral region of the exciton bands a third transition not belonging to the exciton band system was detected.

Keywords. Circular dichroism; Oriented molecules; Dibenzoates; Taddoles; Binaphthols.

* Corresponding author. E-mail: kuball@rhrk.uni-kl.de

Introduction

The *chiroptical analysis* is besides the X-ray diffraction the most established method [1–3] for the determination of the absolute configuration of configurational and conformational chiral compounds. The leading problem is the development of suitable sector and helicity rules or to derive suitable quantum mechanical numerical methods for correlating the sign of the *Cotton* effect (*C*E) of one or more absorption bands with the absolute configuration of a molecule [4] or at least for a chromophore of a molecule. The ''exciton chirality method'' [1] is one of the most outstanding helicity rule, which is based on the quantum mechanical theory of coupled oscillators [5]. Originally developed as the ''dibenzoate chirality method'' [6], the exciton chirality method can be applied to molecules possessing at least two allowed electric dipole transitions positioned in the same spectral region and located in different parts of the molecule. The coupling between at least two electronic transitions leads to two exciton transitions $N_1 \rightarrow K_1$ and $N_2 \rightarrow K_2$ with a CD of different sign, superposing each other to a CD couplet (Fig. 1). The shape, the amplitude and the sign of the couplet are determined by shape and intensity of the two CD bands belonging to $N_1 \rightarrow K_1$ and $N_2 \rightarrow K_2$ of the

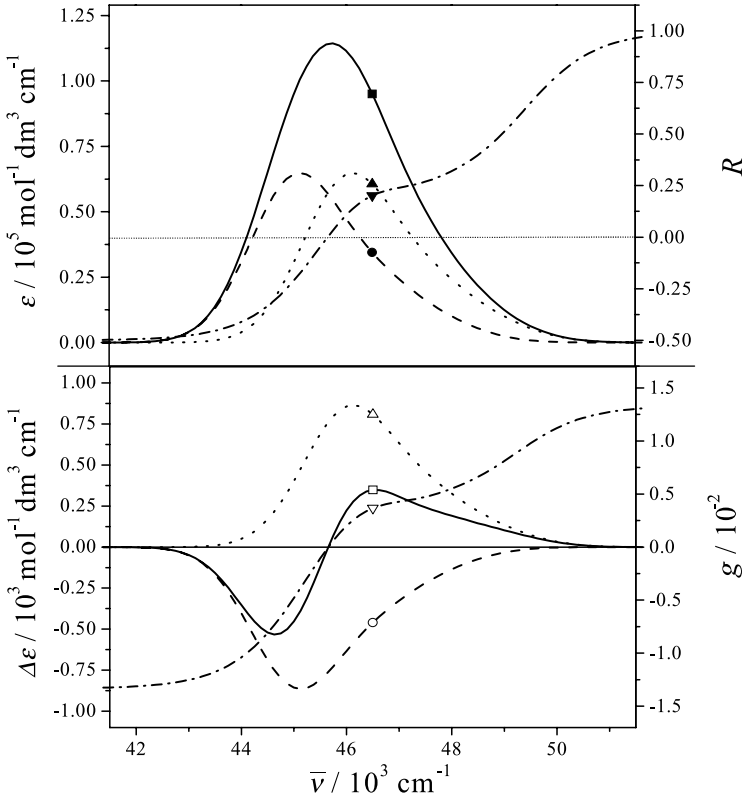

Fig. 1. A *negative* CD couplet (□), the absorption band (■), the dissymmetry factor (▽), and the degree of anisotropy (▼) as a result of a superposition of CD ((○), (△)) and absorption ((●), (▲)) bands belonging to the α (A→B) and β (A→A) exciton transitions of a molecule of C_2 symmetry possessing a *negative chirality* (Appendix A.1)

coupling chromophores and the shift of the energies $E^{\alpha/\beta}$ of the corresponding coupled states [7] (Eq. (1)).

$$E^{\alpha/\beta} = \frac{E_{\mathrm{N_1K_1}} + E_{\mathrm{N_2K_2}}}{2} \mp \frac{1}{2}\sqrt{(E_{\mathrm{N_1K_1}} - E_{\mathrm{N_2K_2}})^2 + 4V_{ij}^2} \tag{1}$$

The integrated intensity of the exciton CD bands is given by their rotational strength (Eq. (2)).

$$R^{\alpha/\beta} = \pm \frac{\pi\bar{\nu}_\mathrm{o}}{2}\vec{R}_{ij} \cdot \langle\vec{\mu}(i)\rangle_{\mathrm{N}_i\mathrm{K}_i} \times \langle\vec{\mu}(j)\rangle_{\mathrm{N}_j\mathrm{K}_j} \tag{2}$$

$\langle\vec{\mu}(q)\rangle_{\mathrm{NK}}$ are the transition moments of transition between the states N and K, located in the chromophores $q = 1, 2, \ldots$. The wavenumber $\bar{\nu}_\mathrm{o}$ is standing for the spectral position of the uncoupled transitions. $\vec{R}_{ij}$ is the intermolecular distance vector between the interacting groups $q = i, j$. V_{ij} is the potential of the dipole–dipole interaction (Eq. (3)).

$$V_{ij} = \frac{1}{|\vec{R}_{ij}|^3}\left[\langle\vec{\mu}(i)\rangle_{\mathrm{N}_i\mathrm{K}_i} \cdot \langle\vec{\mu}(j)\rangle_{\mathrm{N}_j\mathrm{K}_j} - 3\frac{1}{|\vec{R}_{ij}|^2}(\langle\vec{\mu}(i)\rangle_{\mathrm{N}_i\mathrm{K}_i} \cdot \vec{R}_{ij})(\langle\vec{\mu}(j)\rangle_{\mathrm{N}_j\mathrm{K}_j} \cdot \vec{R}_{ij})\right] \tag{3}$$

In a first order approximation the transition moments of the exciton bands are given by Eq. (4). As for Eq. (4), the $-$ and $+$ sign in Eq. (2) conventionally defines the so-called α and β transition.

$$\langle\vec{\mu}\rangle^{\alpha/\beta} = \frac{1}{\sqrt{2}}(\langle\vec{\mu}(i)\rangle_{\mathrm{N}_i\mathrm{K}_i} \mp \langle\vec{\mu}(j)\rangle_{\mathrm{N}_j\mathrm{K}_j}) \tag{4}$$

The integrated intensity, the dipole strength of both electronic transitions, is within this first order approximation given by Eq. (5), *i.e.*, the sum of the intensities of the α and β band is equal to the sum of the intensities of the bands of the coupling undisturbed chromophores. Furthermore, it follows from Eqs. (4) and (5) that the angle between $\langle\vec{\mu}(i)\rangle_{\mathrm{N}_i\mathrm{K}_i}$ and $\langle\vec{\mu}(j)\rangle_{\mathrm{N}_j\mathrm{K}_j}$ determines the intensity ratio D^α/D^β, which is also responsible for the band shape of the CD couplet and the absorption band. The sum of the rotational strength of both exciton bands is equal to zero.

$$D^{\alpha/\beta} = (\langle\vec{\mu}\rangle^{\alpha/\beta})^2. \tag{5}$$

The exciton chirality method has been mostly applied to compounds where both interacting states are approximately degenerated. Even for a larger coupling, the *Davydov* split of the exciton chromophore $2V_{ij}$ leads often to an absorption band possessing only a small shoulder. In contrast to that, the CD spectra possess even then the shape of a couplet (Fig. 1) because the CD bands belonging to the transitions $\mathrm{N}_i \rightarrow \mathrm{K}_i$ and $\mathrm{N}_j \rightarrow \mathrm{K}_j$ are large and opposite in sign. The large CD effect and the characteristic band shape is the origin for the broad applicability of the exciton chirality method [1]. Furthermore, it is of importance that even a simple theory is sufficient to understand and apply this method safely. Most of the fundamental results of the most simple theory can be proven experimentally in spite of the fact that there are theoretical presuppositions needed which are often only very approximately fulfilled.

But there is one problem, in principle. The assignment of the exciton absorption and CD bands, *i.e.*, to assign which band belongs to the α or β transition, is an

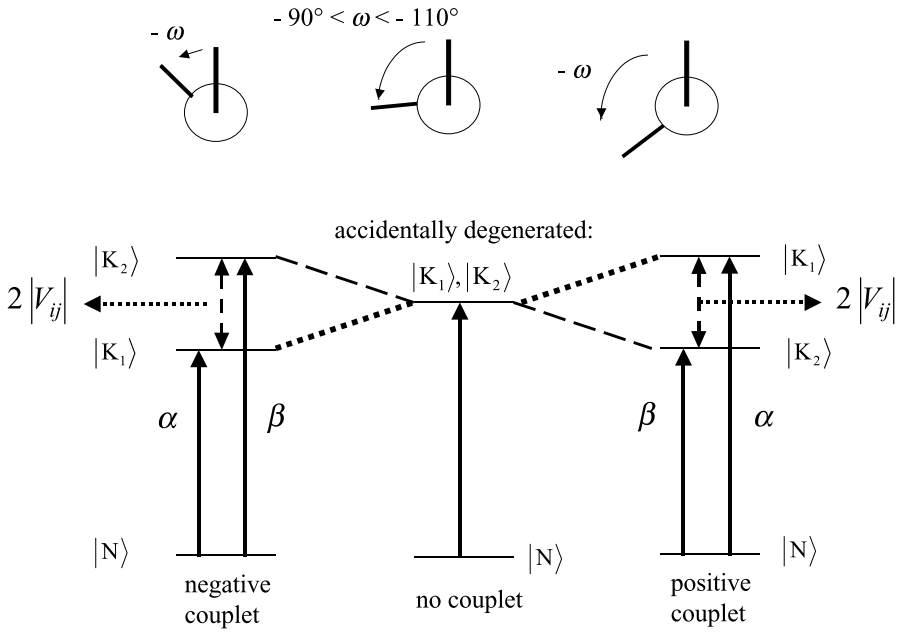

Fig. 2. The change of the term scheme of a binaphthol, possessing *negative chirality*, as a function of the dihedral angle about the naphthyl–naphthyl bond by which the sign of the CD couplet will be inverted without a change of the absolute configuration; the CD of the α (A→B) and β (A→A) transition is, according to Eq. (2), negative and positive for a dihedral angle ω between 0 and $-90°$ to $-110°$; superposition of both CD bands leads to a negative couplet (left-hand side); the couplet is zero if both excited states $|K_1\rangle$ and $|K_2\rangle$ are accidentally degenerated (middle); for ω between $-90°$ to $-110°$ and $-180°$ to $-200°$ a positive couplet results from the CD of the α (A→B) and β (A→A) transition because of the term inversion shown on the right hand side of the figure (Appendix A.1)

unconditional presupposition for a correct application of the exciton chirality method. In many examples this assignment is unequivocally determined by the ordering of the chromophores in a rigid molecule and by approximate calculation of the position of the transitions. But there are examples where an unequivocal assignment is impossible as, *e.g.* for flexible molecules like the (*R*)-1,1′-binaphthols in solution (Fig. 2). A conformational change by increasing the dihedral angle about the naphthyl–naphthyl bond from 60° to 150°, *e.g.*, interchanges the position of the α and β transition in the spectrum and leads to a sign change of the couplet without a change of the absolute configuration. The sign of the linear dichroism, described by the degree of anisotropy, allows a safe assignment of the α and β transition and thus a correct determination of the absolute configuration because exciton bands are differently polarized, in principle. The so-called polarized spectroscopy is a well proven technique to determine transition moment directions [8]. For a few examples such measurements have been done in order to proof the applicability of the exciton chirality method [7].

In addition to the anisotropy of light absorption of oriented or partially oriented molecules there is another optical anisotropy, the anisotropy of circular dichroism (ACD) of anisotropic phases. The ACD spectroscopy is related to the CD as the polarized spectroscopy to the absorption spectroscopy. A first analysis of the ACD

of exciton transitions of molecules dissolved in an anisotropic liquid crystal phase has shown a temperature dependent ratio of the ACD of the two exciton transitions as a function of the order parameters of the dissolved molecules [9]. This paper will present an application of the polarized and ACD spectroscopy to compounds possessing exciton transitions in order to obtain further and new informations about inherent dissymmetric chromophores. For such a discussion, CD ($\Delta\varepsilon$), the ACD ($\Delta\varepsilon^{A}$) spectra, the degree of anisotropy (R), and the quadrupole NMR spectra of deuterated species have to be available.

Working Equations

Circular Dichroism of an Anisotropic Sample

Optical activity with its circular dichroism $\Delta\varepsilon$ and its optical rotation [M] yields pseudoscalar quantities. Pseudoscalar results have to change sign for the mirror image of the system. A theoretical description of the CD of an anisotropic phases ($\Delta\varepsilon^{A}$) requires beside pseudoscalars also pseudotensors of second rank like those given in Eq. (6).

$$\Delta\varepsilon^{A} = \Delta\varepsilon_{33} \tag{6}$$

The tensor coordinate $\Delta\varepsilon_{33}$ is the circular dichroism of an ensemble of molecules ordered rotationally symmetric about the propagation direction of the measuring light beam which is chosen here as the x_3 direction (Appendix A.2). The mean value of three analogous measurements along three mutually perpendicular axes yields the CD of an isotropic phase[a)] (Eq. (7)).

$$\Delta\varepsilon = \frac{1}{3}(\Delta\varepsilon^{*}_{11} + \Delta\varepsilon^{*}_{22} + \Delta\varepsilon^{*}_{33}) \tag{7}$$

For an anisotropic phase with partially oriented molecules the CD measurement, the ACD, along the optical axis of a uniaxial phase results in Eq. (8) where g_{ij33} are the coordinates of the order tensor, $\Delta\varepsilon^{*}_{ii}$ are the coordinates of the CD tensor given with respect to the principal axes of the order tensor, and $\Delta\varepsilon^{o}_{ii}$ are the coordinates given in its own principal axes (Appendix A.2). The subscripts of $\Delta\varepsilon_{ii}$ indicate the coordinate axis x_i along which the measuring light beam propagates. The a_{ij} are the elements of the transformation matrix for a transformation from the principal axes of the order tensor to the principal axes of the CD tensor [11]. Non-diagonal elements of $\Delta\varepsilon_{ij}$ $(i \neq j)$ can only be avoided in Eq. (8) when either the order tensor or the circular dichroism tensor is given in its principal axes (Eq. (9)).

$$\Delta\varepsilon^{A} = \sum_{i=1}^{3}\sum_{j=1}^{3} g_{ij33}\Delta\varepsilon_{ij} = \sum_{i=1}^{3} g^{*}_{ii33}\Delta\varepsilon^{*}_{ii} = \sum_{i=1}^{3} a^{2}_{ij}g^{*}_{jj33}\Delta\varepsilon^{o}_{ii} \tag{8}$$

$$\Delta\varepsilon^{A} = g^{*}_{1133}\Delta\varepsilon^{*}_{11} + g^{*}_{2233}\Delta\varepsilon^{*}_{22} + g^{*}_{3333}\Delta\varepsilon^{*}_{33} \tag{9}$$

The coordinates of the order tensor g_{ij33} ($i,j = 1,2,3$; g_{ijkl} orientation distribution coefficients) are measures of the orientational distribution of molecules in anisotropic

[a)] One has to take care that only the ''chiral part'' of measured quantities is taken into account [10]

phases. x_i^* $(i=1,2,3)$ are the principal axes of the order tensor g_{ii33}^* (Appendix A.3). In liquid crystal science mostly the more convenient order parameters of *Saupe S* and D (Eq. (10)) are used to describe the order of molecules in uniaxial phases. For the description of the ACD these order parameters can only be used under suitable conditions.

$$S^* = \frac{1}{2}(3g_{3333}^* - 1), \quad \text{and} \quad D^* = \frac{\sqrt{3}}{2}(g_{2233}^* - g_{1133}^*) \tag{10}$$

The ACD of a uniaxial phase of a light beam propagating parallel to the optical axis can then be given by Eq. (11) where $0 \leq S^* \leq 1$ and $0 \leq D^* \leq \frac{\sqrt{3}}{2}$ (Appendix A.3). By the convention for the numbering of the axes of the coordinate system (Eq. (12)) the so-called orientation axis (x_3^* axis) for a molecule can be introduced. This is the best ordered axis of the molecule, *i.e.*, the axis to which the largest order parameter S belongs.[b] The price for the simplicity of the description of the ACD by Eq. (11) is paid by the problem that the description is only unequivocally when the coordinate system to which the order parameters S and D belong is known. Often this coordinate system depends on the method with which the order parameters have been determined [12]. To be independent of any molecular property as, *e.g.*, the transition moment direction *etc.*, the coordinates of the order tensor g_{ij33} $(i=1,2,3)$ have to be given with respect to their principal axes (Appendix A.3).

$$\Delta\varepsilon^{\mathrm{A}} = \Delta\varepsilon + (\Delta\varepsilon_{33}^* - \Delta\varepsilon)S^* + \frac{1}{\sqrt{3}}(\Delta\varepsilon_{22}^* - \Delta\varepsilon_{11}^*)D^* \tag{11}$$

$$g_{3333}^* \geq g_{2233}^* \geq g_{1133}^* \tag{12}$$

To measure the CD with a light beam propagating perpendicular to the optical axis of a uniaxial phase ($\Delta\varepsilon^{\mathrm{A}}$) or in any arbitrary direction is a very difficult task and can only be done in a reliable way with specialized equipments [13]. Under these experimental situations an elliptical birefringence and elliptical dichroism is obtained. These quantities are of ''mixed symmetry'' and, thus, are determined by achiral and chiral effects.[c] Therefore, these results have to be decomposed into a chiral ($\Delta\varepsilon_2^{\mathrm{A}}$) and an achiral contribution.[d] If $\Delta\varepsilon^{\mathrm{A}}$ and $\Delta\varepsilon$ can be measured for one and the same temperature, $\Delta\varepsilon_2^{\mathrm{A}}$ can be evaluated for uniaxial phases by the relation given with Eq. (13).

$$\Delta\varepsilon = \frac{1}{3}(\Delta\varepsilon^{\mathrm{A}} + 2\Delta\varepsilon_2^{\mathrm{A}}) \tag{13}$$

With these two chirality measurements $\Delta\varepsilon^{\mathrm{A}}$ and $\Delta\varepsilon_2^{\mathrm{A}}$ the ACD of the uniaxial phase is completely determined. Any result of chirality measurements with light beams propagating into oblique directions can be calculated presupposed that the ''achiral parts'' of the measured effects are suppressed. *In this paper only ACD measurements*

[b] The size of S and D varies when different molecule-fixed coordinate systems are chosen for the description of S and D [12]

[c] Chiral $\leftrightarrow$ pseudoscalar quantities and achiral $\leftrightarrow$ scalar quantities

[d] In a systematic nomenclature $\Delta\varepsilon^{\mathrm{A}}$ should be named $\Delta\varepsilon_1^{\mathrm{A}}$

along the optical axis and CD measurements with isotropic phases have been considered, which are sufficient to determine the CD tensor on the assumption that the CD ($\Delta\varepsilon$) is temperature independent within a temperature range slightly higher than the phase transition temperature and the temperature of the ACD measurement.

Anisotropic Absorption of an Anisotropic Sample

To characterize the optical properties of anisotropic samples the determination of the anisotropic absorption is recommended. The linear dichroism for a uniaxial phase is obtained from the difference of absorption coefficients measured with light beams which are polarized parallelly and perpendicularly to the optical axis (ε_1, ε_2). Equations (14) and (15) hold for these beams propagating perpendicularly to this axis.

$$\varepsilon_k = \sum_{i,j} g_{ijkk}\varepsilon_{ij} = \sum_{i,j} a_{ij}^2 g_{jjkk}^{*}\varepsilon_{ii}^{+} \quad (k = 1, 2) \tag{14}$$

$$\varepsilon_1 = \varepsilon + (\varepsilon_{33}^{*} - \varepsilon)S^{*} + \frac{1}{\sqrt{3}}(\varepsilon_{11}^{*} - \varepsilon_{22}^{*})D^{*} \tag{15}$$

$\varepsilon_{ii}^{\#}$ are the coordinates of the absorption tensor ($\# = {}^{*}, +$). The symbols $+$ and * indicate that the tensor coordinates are given with respect to their own principle axes or in the principle axis of the order tensor, respectively. a_{ij} are the elements of the transformation matrix [11] from the * into the $+$ coordinate system. The absorption coefficient of an unpolarized light beam propagating perpendicularly to the optical axis is given by Eq. (16) whereas the absorption coefficient for the corresponding isotropic phase is described by Eq. (17).

$$\bar{\varepsilon} = \frac{1}{2}(\varepsilon_1 + \varepsilon_2) \tag{16}$$

$$\varepsilon = \frac{1}{3}(\varepsilon_1 + 2\varepsilon_2) = \frac{1}{3}(\varepsilon_{11}^{+} + \varepsilon_{22}^{+} + \varepsilon_{33}^{+}) \tag{17}$$

The degree of anisotropy R is a very convenient quantity to describe the linear dichroism $\varepsilon_1 - \varepsilon_2$ of a uniaxial phase [8] (Eq. (18)) with q_{ij} given by Eq. (19).

$$R = \frac{\varepsilon_1 - \varepsilon_2}{\varepsilon_1 + 2\varepsilon_2} = \frac{\varepsilon_1 - \varepsilon_2}{3\varepsilon} == \frac{1}{2}\sum_{i,j}(3g_{ij33} - \delta_{ij})q_{ij} \tag{18}$$

$$q_{ij} = \frac{\varepsilon_{ij}}{\sum_i \varepsilon_{ii}} = \frac{\varepsilon_{ij}}{3\varepsilon} \tag{19}$$

In earlier literature [8] often the degree of polarization P has been introduced instead of R: $R = 2P/(3 - P)$ ($\cong 2P/3$ for small P). The degree of anisotropy is easier to handle than the linear dichroism $\varepsilon_1 - \varepsilon_2$ or the degree of polarization because its denominator is 3ε, *i.e.*, a pure number. R is a measure for the transition moment direction within the molecules. The elements of the absorption tensor are a generalized description for products of the coordinates of the transition moments $\mu_i : \varepsilon_{ij} \propto \mu_i\mu_j$. The subscripts of the diagonal elements ε_{ii} indicate the coordinate axis x_i along which the measuring light beam has to be polarized (Appendices A.4 and A.5).

Rotational and Dipole Strength

Any spectrum possesses two kinds of information, namely the intensity of the total band and its spectral band shape. Often only the total intensity is of interest which is described by the rotational strength (Eq. (20)) for the CD and the optical rotation and the dipole strength (Eq. (22)) for the absorption belonging to the transition $|0\rangle \rightarrow |\mathrm{n}\rangle$.

$$R^{0\mathrm{n}} = \frac{3}{B}\int_{\text{band } 0\rightarrow \mathrm{n}} \frac{\Delta\varepsilon^{0\mathrm{n}}(\bar{\nu})}{\bar{\nu}}\,\mathrm{d}\bar{\nu} = \mathrm{Im}\{\langle\vec{\mu}\rangle_{0\mathrm{n}} \cdot \langle\vec{m}\rangle_{\mathrm{n}0}\} = \sum_{i=1}^{3} \mathrm{Im}\{\langle\mu_i\rangle_{0\mathrm{n}}\langle m_i\rangle_{\mathrm{n}0}\} \quad (20)$$

$$B = \frac{32\pi^3 \mathrm{N_A}}{10^3 \mathrm{hc}\ln 10}; \quad \frac{3}{B} = 22.96 \cdot 10^{-40}\,\mathrm{cgs} \quad (21)$$

$$D^{0\mathrm{n}} = \frac{12}{B}\int_{\text{band } 0\rightarrow n} \frac{\varepsilon^{0\mathrm{n}}(\bar{\nu})}{\bar{\nu}}\,\mathrm{d}\bar{\nu} \quad (22)$$

$\mathrm{Im}\{\ldots\}$ is the imaginary part of $\{\ldots\}$. The rotational strength and the dipole strength of the isotropic state are equal to one third of the trace of the circular dichroism (CD) tensor (Eq. (23)) and the trace of the absorption tensor (Eq. (24)).

$$\Delta\varepsilon_{ij} = B\bar{\nu}\sum_{0,\mathrm{n}} R_{ij}^{0\mathrm{n}} G^{0\mathrm{n}}(\bar{\nu}) \quad (23)$$

$$\varepsilon_{ij} = \frac{B\bar{\nu}}{4}\sum_{0,\mathrm{n}} D_{ij}^{0\mathrm{n}} F^{0\mathrm{n}}(\bar{\nu}) \quad (24)$$

The rotational strength tensor $R_{ij}^{0\mathrm{n}}$ and the transition moment tensor $D_{ij}^{0\mathrm{n}}$ for the transition $|0\rangle \rightarrow |\mathrm{n}\rangle$ are given by Eqs. (25) and (26).

$$R_{ij}^{0\mathrm{n}} = \frac{1}{4}\sum_{k,l}\langle\mu_k\rangle_{0\mathrm{n}}(\varepsilon_{kli}\langle C_{lj}\rangle_{\mathrm{n}0} + \varepsilon_{klj}\langle C_{li}\rangle_{\mathrm{n}0}) \quad (25)$$

$$D_{ij}^{0\mathrm{n}} = \langle\mu_i\rangle_{0\mathrm{n}}\langle\mu_j\rangle_{\mathrm{n}0} \quad (26)$$

$G^{0\mathrm{n}}(\bar{\nu})$ and $F^{0\mathrm{n}}(\bar{\nu})$ are the band shapes, the spectral functions, for the CD and UV bands for the transitions $|0\rangle \rightarrow |\mathrm{n}\rangle$. They are equal for most cases of application. $\sum_{0,\mathrm{n}}$ is the sum over all electronic (N, K) and vibrational states (n, k): $0 \equiv \mathrm{Nn}$ and $\mathrm{n} \equiv \mathrm{Kk}(\sum_{\mathrm{NnKk}})$. $\langle C_{ij}\rangle_{\mathrm{n}0}$ is a sum of the magnetic dipole and electric quadrupole transition moment contributing to the CD (Eqs. (27) and (28)). $\langle\mu_i\rangle_{0\mathrm{n}}$, $\langle m_i\rangle_{\mathrm{n}0}$, and $\langle Q_{ij}\rangle_{\mathrm{n}0}$ are the coordinates of the electric dipole, the magnetic dipole, and the electric quadrupole transition moment: $\langle Q_{ij}\rangle = \langle Q_{ji}\rangle$. ε_{ijk} are the coordinates of the *Cevi-Levita* tensor ($\varepsilon_{123} = \varepsilon_{312} = \varepsilon_{231} = 1$; $\varepsilon_{132} = \varepsilon_{213} = \varepsilon_{321} = -1$; all other coordinates are equal to zero). The $\langle C_{ij}\rangle_{\mathrm{n}0}$ cannot be decomposed into origin independent quantities, in general (Appendix A.5) [14].

$$\langle C_{31}\rangle_{\mathrm{n}0} = -\mathrm{i}\langle m_2\rangle_{\mathrm{n}0} - \frac{\omega_{\mathrm{n}0}}{\mathrm{c}}\langle Q_{31}\rangle_{\mathrm{n}0} \quad (27)$$

$$\langle C_{13}\rangle_{\mathrm{n}0} = \mathrm{i}\langle m_2\rangle_{\mathrm{n}0} - \frac{\omega_{\mathrm{n}0}}{\mathrm{c}}\langle Q_{13}\rangle_{\mathrm{n}0} \quad (28)$$

$\langle C_{12}\rangle_{n0}$ and $\langle C_{23}\rangle_{n0}$ can be obtained by cyclic permutation of the indices of $\langle C_{31}\rangle_{n0}$ whereas $\langle C_{21}\rangle_{n0}$ and $\langle C_{32}\rangle_{n0}$ are analogously obtained from $\langle C_{13}\rangle_{n0}$. $\omega_{n0} = (E_n - E_0)/\hbar$. E_0 and E_n are the energies of the states $|0\rangle$ and $|n\rangle$ and c is the velocity of light in the vacuum. For the anisotropic system a tensorial rotational strength R^T (Eq. (29)) has been defined as an experimental quantity which, in contrast to R^{0n} (Eq. (20)), is also determined by the order of the system, *i.e.*, contains molecular and phase parameters.

$$R^T = \frac{1}{B}\int_{band} \frac{\Delta\varepsilon^A(\bar{\nu})}{\bar{\nu}}\,d\bar{\nu} = \sum_{i,j} g_{ij33}R^{0n}_{ij} \tag{29}$$

Furthermore, a rotational strength for a tensor coordinate *ij* can be derived (Eq. (29)) which is an order independent quantity and thus, equivalent to R^{0n} (Eq. (30)).

$$R^{0n}_{ij} = \frac{1}{B}\int_{band} \frac{\Delta\varepsilon_{ij}(\bar{\nu})}{\bar{\nu}}\,d\bar{\nu} \tag{30}$$

With the help of the rotational strength and the dipole strength, *Kuhn*'s dissymmetry factor [1] can be defined by Eq. (31) which corresponds to the wavelength dependent dissymmetry factor given by Eq. (32).

$$g = \frac{4R^{0n}}{D^{0n}} \tag{31}$$

$$g(\bar{\nu}) = \frac{\Delta\varepsilon^{0n}(\bar{\nu})}{\varepsilon^{0n}(\bar{\nu})} \tag{32}$$

These quantities allow to classify the transitions belonging to the CD bands [3].

ACD of the Exciton Transitions

The exciton model requires at least two coupled transitions localized in different groups of the molecule which are suitably oriented against each other. The two evolved exciton transitions of molecules of C_2 symmetry are mutually perpendicularly polarized with respect to each other. For molecules without any symmetry a distinct angle between the transition moment directions of the exciton transitions exists. This opens a chance for the ACD spectroscopy to analyze exciton transitions because they can be observed separately also when their bands totally overlap, *i.e.*, if V_{ij} is very small. Assuming as an example exciton transitions polarized in the x_1 and x_2 direction ($\langle\mu_1\rangle_{0n} \neq 0$, $\langle\mu_2\rangle_{0n} \neq 0$), then immediately follows from Eqs. (33)–(35) that the spectrum of $\Delta\varepsilon_{33} \neq 0$ exhibits a couplet whereas $\Delta\varepsilon_{11} \neq 0$ and $\Delta\varepsilon_{22} \neq 0$ are determined only by the x_2 ($\langle\mu_2\rangle_{0n} \neq 0$) and only by the x_1 ($\langle\mu_1\rangle_{0n} \neq 0$) polarized exciton transition. Thus, it makes sense to divide the compounds with an exciton spectrum into two classes by their symmetry if the ACD spectroscopy will be applied as an additional part of the exciton chirality method:

(A) Molecules without any symmetry possess exciton transitions which are polarized in any arbitrary direction. A quantitative discussion of the effect of these molecules is difficult without a quantum mechanical calculation of the dipole and quadrupole transition moments [15–17]. Furthermore, the orientation of the principal axes of the order tensor and thus, also the orientation axis, is not fixed by symmetry and can be oriented in any direction of the molecule. In addition to this, all principal axes of other tensors (Appendix A.2) are oriented arbitrarily and have to be determined experimentally.

(B) Chiral molecules with a C_n symmetry. The axis parallel to the C_n rotation axis for these molecules is one of the principal axes of the order tensor, the tensor of absorption as well as the tensor of rotation (gyration tensor).

$$\Delta\varepsilon_{11}(\bar{\nu}) = \frac{1}{2}B\bar{\nu}\sum_{n}\{\langle\mu_2\rangle_{0n}\langle C_{31}\rangle_{n0} - \langle\mu_3\rangle_{0n}\langle C_{21}\rangle_{n0}\}G^{0n}(\bar{\nu}), \tag{33}$$

$$\Delta\varepsilon_{22}(\bar{\nu}) = \frac{1}{2}B\bar{\nu}\sum_{n}\{\langle\mu_3\rangle_{0n}\langle C_{12}\rangle_{n0} - \langle\mu_1\rangle_{0n}\langle C_{32}\rangle_{n0}\}G^{0n}(\bar{\nu}), \tag{34}$$

$$\Delta\varepsilon_{33}(\bar{\nu}) = \frac{1}{2}B\bar{\nu}\sum_{n}\{\langle\mu_1\rangle_{0n}\langle C_{23}\rangle_{n0} - \langle\mu_2\rangle_{0n}\langle C_{13}\rangle_{n0}\}G^{0n}(\bar{\nu}) \tag{35}$$

Results and Discussions

Dibenzoates

α-Glycosidic dibenzoates (Scheme 1), substituted with suitable groups R^i ($i = 1, 2, 3$), are very effective dopants for the chiral induction of cholesteric phases. Especially, the dibenzoate (*S*)-**1**, *e.g.*, is a suitable aspirant for twisted nematic (TN) cells in the display technology [18, 19] because of its huge helical twisting power (*HTP*), which is temperature independent over a large range of temperature. The large *HTP* and the temperature independence are not well understood and explainable only by contradictory assumptions. A helical instead of an elongated structure of conformers of (*S*)-**1** with a pronounced ''form chirality'' of the dopant may be

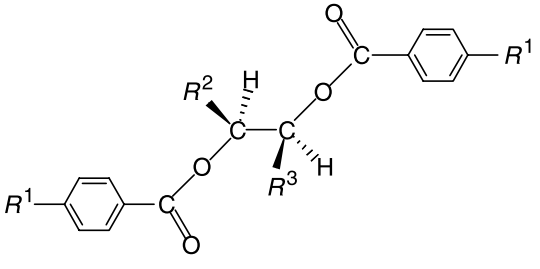

R^1 = 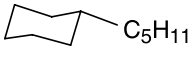 C_5H_{11} $\quad$ R^2 =  $\quad$ R^3 = H

(*S*)-**1**

Scheme 1

the origin of the extremely large *HTP* effect. Helical conformers are accessible by the free rotation about C–C bonds in the aliphatic chain of (*S*)-**1**. The existence of various equilibria of conformers have been proven for related compounds [20] by NMR studies. But as a consequence temperature dependent molecular properties should be expected which are not found with (*S*)-**1**. The CD couplet in *n*-heptane and in the isotropic ZLI-1695 as well as the *HTP* is temperature independent for the dibenzoate (*S*)-**1** in a temperature range between 20° to 80°C. The *Moscowitz* method [21], analyzing the CD as a function of *T via* the *Boltzmann* factor, yields a contribution of different conformers less than 1% to the CD spectrum [22]. An explanation that all involved conformers in solution are of equal energy is not very plausible.

A hint for at least one conformer possessing a helical structure is the CD spectrum itself with its couplet like dispersion in the spectral region of the charge transfer transition of the two benzoate groups (35000 and 45000 cm^{-1}, 285 to 220 nm, [22]). This assignment is further supported by 1) in mono-benzoates of the same structure only simple CD spectra have been found in the spectral region of the charge transfer transition, 2) the wavenumber dependence of the degree of anisotropy in the corresponding spectral region establishes two differently polarized transitions (Fig. 4).

The temperature variation of the shape of the couplet of the ACD spectrum (Fig. 3) has to have its origin in the temperature dependence of the orientational order of (*S*)-**1** for two reasons: 1) the variation of the shape is developing parallel to the variation of the degree of anisotropy, and 2) no temperature variation of an equilibrium of conformers has been found in organic solvents and especially not in the isotropic phase of ZLI-1695. Thus, disappearing of the higher-wavenumber peak of the couplet with decreasing temperature (Fig. 3) has to be an effect of the large anisotropy of the

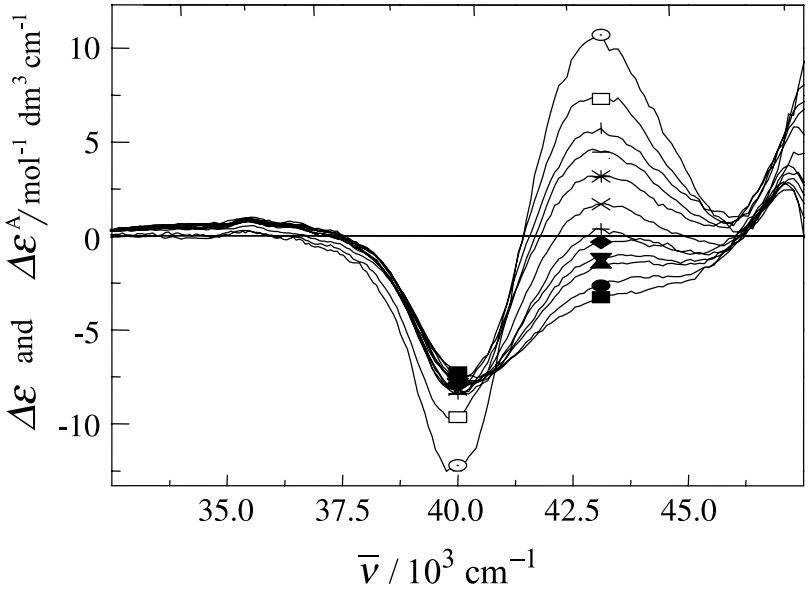

Fig. 3. The circular dichroism $\Delta\varepsilon$ (⬭) at $T = 80$°C in the isotropic phase of ZLI-1695 and $\Delta\varepsilon^{A}$ of the dibenzoate (*S*)-**1** at $T = 28$ (■), 43 (●), 53 (▲), 58 (▼), 61 (◆), 65 (+), 67.5 (×), 68.5 (✳), 69.5 (–), 70 (|), and 70.5°C (▭); concentration in the isotropic phase of ZLI-1695: $1.867 \cdot 10^{-3}$ mol dm^{-3} [22]

CD tensor belonging to the exciton transitions. Because the orientation of the molecules and by this the orientation of the transition moment direction of the exciton transitions varies with respect to the propagation direction of the light $\Delta\varepsilon^{A}$ changes as discussed in the preceding section. This conclusion is also supported by the fact that the couplet does not disappear for a compound where $R^1 = H$ [22] because the variation of orientational order of this compound in the LC phase is too small.

It is more than difficult to derive conclusions with the exciton chirality method for flexible molecules. But it is possible to receive new informations if data from the polarized spectroscopy and the ACD are accessible. An exciton chromophore of approximately C_2 symmetry is produced if the two benzoate groups of (*S*)-**1** build up a conformer with a helical structure. The exciton transitions are then polarized approximately perpendicular to each other. The sign of the corresponding couplet depends on the handedness of the conformer but also on the angle ϑ between the transition moments of both charge transfer transitions of the dibenzoate chromophores. From the negative couplet of (*S*)-**1** with its negative first[e)] and positive second *Cotton* effect results a negative chirality of the conformer if $\vartheta < 90°$ and a positive chirality if ϑ lies between 90° and 180°. But for the assignment of the sign of the chirality for (*S*)-**1**, *i.e.* of the negative couplet, as depicted in Fig. 3, the question arises whether the A→A (β) or the A→B (α) transition is located at lower or higher wavenumbers. The degree of anisotropy of (*S*)-**1** is a few percent larger at the lower wavenumber side – longer wavelengths side – of the

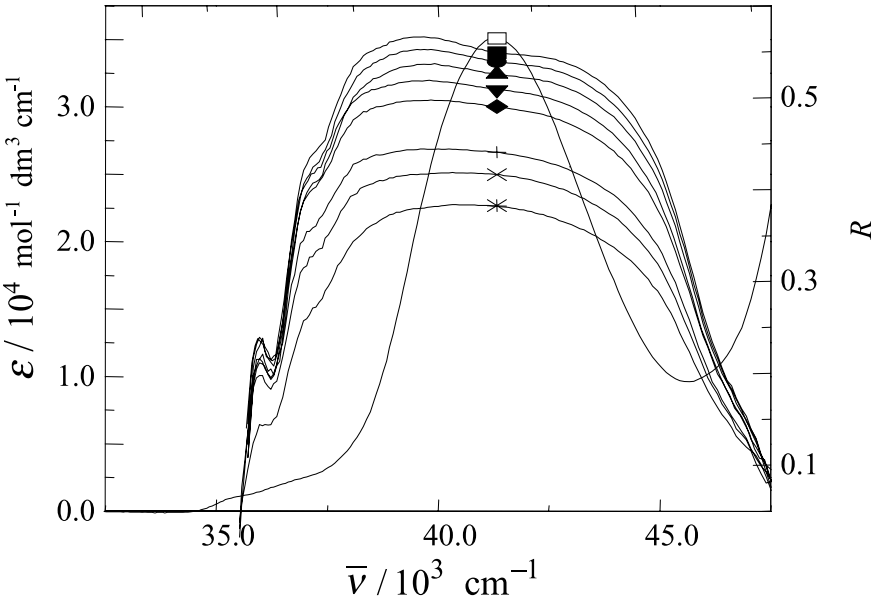

Fig. 4. Molar decadic absorption coefficient (□) of the dibenzoate (*S*)-**1** at $T = 80°C$ in the isotropic phase of ZLI-1695 and the degree of anisotropy in the nematic phase of ZLI-1695 at temperatures $T = 28$ (■), 33 (●), 38 (▲), 43 (▼), 48 (◆), 58 (+), 61 (×), and 65°C (✳) [22]

[e)] In Fig. 2 a wavenumber scale is used and therefore one has to write that a negative *Cotton* effect at smaller wavenumbers and a positive *Cotton* effect at larger wavenumbers belongs to a structure with negative chirality

unstructured band (Fig. 4). Therefore, the angle between the transition moment of the long-wavelength band and the orientation axis is smaller than the angle of the short-wavelength transition and the orientation axis. The determination of the orientation of the orientation axis within the molecule is a difficult task because of the diversity of structures of the conformations of (*S*)-**1** with its four degrees of freedom of rotation about the C–C bonds in the aliphatic chain. Additional information can be obtained from the ACD where the higher wavenumber couplet disappears with increasing long-range orientational order. According to Eq. (9) the ACD values $\Delta\varepsilon^{A}$ converge against $\Delta\varepsilon^{*}_{33}$ if g^{*}_{3333} converge against 1. On this condition $\Delta\varepsilon^{*}_{33} \rightarrow 0$ for (*S*)-**1** in the short-wavelength exciton transition (Fig. 3). The tensor coordinate $\Delta\varepsilon^{*}_{33}$ is equal to zero for two cases, namely $\langle\mu^{*}_{1}\rangle_{0n} = \langle\mu^{*}_{2}\rangle_{0n} = 0$ or $\langle\mu^{*}_{1}\rangle_{0n}\langle C^{*}_{23}\rangle_{n0} \cong \langle\mu^{*}_{2}\rangle_{0n}\langle C^{*}_{13}\rangle_{n0}$. In the first case the short-wavelength transition is polarized in the x^{*}_{3} direction and the degree of anisotropy R of this band has to be larger than R for the long-wavelength band. This is in contradiction to the experimental result for (*S*)-**1**. In the second case the short-wavelength transition is polarized in the $x^{*}_{1}x^{*}_{2}$ plane. Then the long-wavelength transition has to be polarized either also in the $x^{*}_{1}x^{*}_{2}$ plane with a smaller angle to the x^{*}_{2} axis than the short-wavelength transition or in the $x^{*}_{1}x^{*}_{3}$ or $x^{*}_{2}x^{*}_{3}$ plane or parallel to the x^{*}_{3} axis because R is larger in the region of the long-wavelength side of the absorption band (Fig. 4). Because of the assumed C_2 symmetry both exciton transitions are polarized perpendicularly to each other. Thus, a polarization of the short-wavelength band parallel to the x^{*}_{1} direction can be excluded because $R > 0$. Thus, one can assume with high probability that the short wavelength transition is polarized in the $x^{*}_{1}x^{*}_{2}$ plane with a direction in between both axes x^{*}_{1} and $x^{*}_{2}$and the long-wavelength band is parallel to the x^{*}_{3} axis. If this conclusion is allowed then the long-wavelength and the short-wavelength band are of A→A and of A→B symmetry, respectively. *I.e.*, the orientation of both benzoate groups includes an angle ω between 90 and 180° and, therefore to the negative couplet belongs a conformer of positive chirality. The size of the amplitude of the couplet of (*S*)-**1** needs then an interchromophoric distance R_{ij} similar to those of the benzoates of cyclic α-glycols [23]. The interchromophoric distance R_{ij} for (*S*)-**1** is of an acceptable size. The stretched structure of the conformer with ω between 90 and 180° leads to a length to breadth ratio which is consistent with an order parameter $R \cong S \cong 0.5$. But one problem is left. Both enantiomers of the assumed conformations are very similar in their total energy and thus, approximately in a 1:1 ratio. The size of the amplitude of the couplet and the *HTP* is probably too large for the here expected small excess of one of the enantiomers. Therefore, further experimental and theoretical studies are needed to solve this interesting problem.

Taddoles

The taddoles (Scheme 2) are examples for compounds with more than two exciton transitions. For many of the analyzed taddoles with their, at least, four exciton transitions one simple couplet has been observed in the spectral region of the $^{1}B_{b}$ transition of naphthalene [24]. The amplitudes of the CD of (*R*,*R*)-**2** and (*S*,*S*)-**3** are strongly temperature dependent varying from -294 and $+484\,\mathrm{mol^{-1}\,dm^{3}\,cm^{-1}}$ at 5°C to -175 and $+344\,\mathrm{mol^{-1}\,dm^{3}\,cm^{-1}}$ at 75°C, which shows conformational changes as

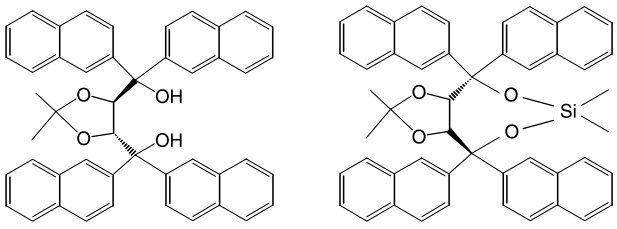

(*R,R*)-**2** (*S,S*)-**3**

Scheme 2

expected from MM2 calculations [25]. Both taddoles, chosen here as examples, exhibit similar spectra in the isotropic state – except that they are enantiomers. The ACD spectrum of (*R,R*)-**2** shows also a single couplet. The temperature dependence of this couplet resembles the temperature dependence of the CD of the isotropic solution. The second example (*S,S*)-**3** was chosen in order to demonstrate how different the behavior of two similar taddoles can be. Whereas $\Delta\varepsilon^{A}$ and $\Delta\varepsilon$ for (*R,R*)-**2** are given by simple very similar couplets, $\Delta\varepsilon^{A}$ and $\Delta\varepsilon$ of (*S,S*)-**3** possess couplets of different sign. Beside a change of the amplitude also the intensity and shape of the couplet of (*S,S*)-**3** varies as a function of temperature which have to be its origin in a conformational change as well as a variation of the orientational order. In both cases the behavior of the exciton bands is very complex and not understood, until now [24, 26].

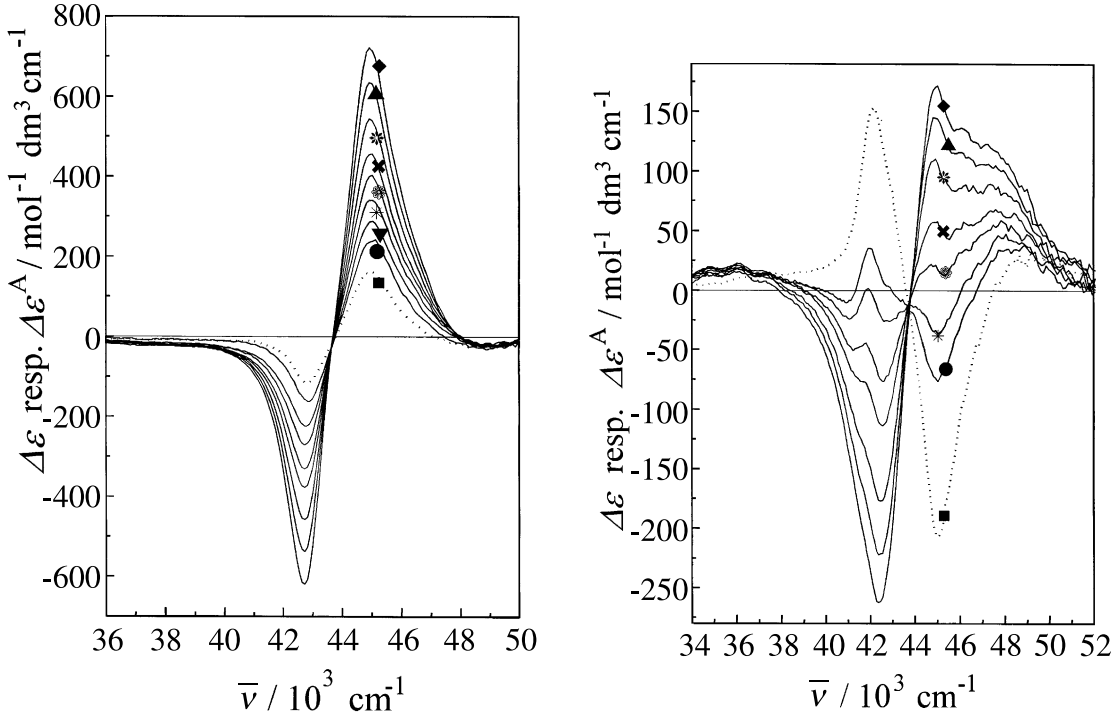

Fig. 5. CD-spectra (···) at $T = 80°C$ (■) and the ACD-spectra (—) of (*R,R*)-**2** (left) and of (*S,S*)-**3** (right) at $T = 28$ (◆), 38 (▲), 48 (❋), 58 (×), 63 (❁), 68 (✳), 70.5 (▼), and 71°C (●) in ZLI-1695

Binaphthols – UV Absorption Spectroscopy and the Degree of Anisotropy

The binaphthols of Scheme 3 possess, at least approximately, a C_2 symmetry. Their two exciton transitions, originated by the coupling of the ^1B_b transitions of the naphthyl chromophores, are polarized parallel to the C_2 rotation axis (x_1 axis, A→A transition) and in the plane perpendicular to the diadic rotation axis (x_2x_3 plane; x_3 axis parallel to the naphthyl–naphthyl bond: A→B transition). There are two questions to be answered: 1) Belongs the long-wavelength or the short-wavelength band to the A→A or A→B transition? 2) What is the orientation of the principal axes of the order tensor with respect to the molecular skeleton taking into account the convention Eq. (12)?

The orientation of the principal axes of the order tensor of (*R*)-**4** and (*R*)-**6** to (*R*)-**10** in the liquid crystal phase ZLI-1695 has been determined by ^2H NMR spectroscopy [27]. Neglecting deviations between 0 to 14° the orientation of the axes are: (*R*)-**4**: all x_i^* parallel to x_i; (*R*)-**6**: x_1^* axis parallel to x_1, x_3^* antiparallel to x_2, x_2^* parallel to x_3; (*R*)-**7** to (*R*)-**9**: x_2^* axis parallel to x_1, x_1^* axis antiparallel to x_2, x_3^* axis parallel to x_3; and (*R*)-**10**: x_3^* axis parallel to x_1, x_1^* axis parallel to x_2, x_2^* axis parallel to x_3. The orientation axis (the x_3^* axis by definition) can be oriented parallel to the C_2 symmetry axis or in any direction within the plane perpendicular to the C_2 symmetry axis, in principle.

Whereas the *Davydov* splitting of the bridged binaphthols (*R*)-**7** to (*R*)-**10** leads to an absorption band with a shoulder (Fig. 6), for the unbridged binaphthols nearly no broadening of the absorption bands can be detected (Fig. 7). The degree of anisotropy *R* of (*R*)-**8** and (*R*)-**10** increases from positive values and for (*R*)-**7** and (*R*)-**9** from a negative minimum at the long-wavelength side towards larger positive values at the short-wavelength side of the absorption band. A positive degree of anisotropy can only be obtained for transitions polarized – using the convention Eq. (12) – along the x_2^* and x_3^* axes. Because both exciton transitions are perpendicularly polarized with respect to each other, the short-wavelength transition of (*R*)-**8** is polarized perpendicularly and of (*R*)-**10** parallelly to the orientation axis. Thus, the short-wavelength transition is of A→A symmetry in

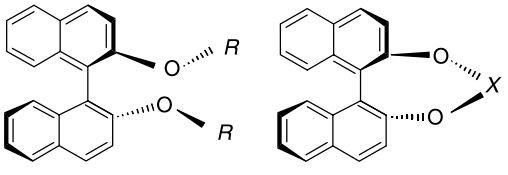

R = H ((*R*)-**4**), CH_3 ((*R*)-**5**), $CH(CH_3)_2$ ((*R*)-**6**); *X* = CH_2 ((*R*)-**7**), Si(*t*-*Bu*)$_2$ ((*R*)-**8**)

((*R*)-**9**) ((*R*)-**10**)

Scheme 3

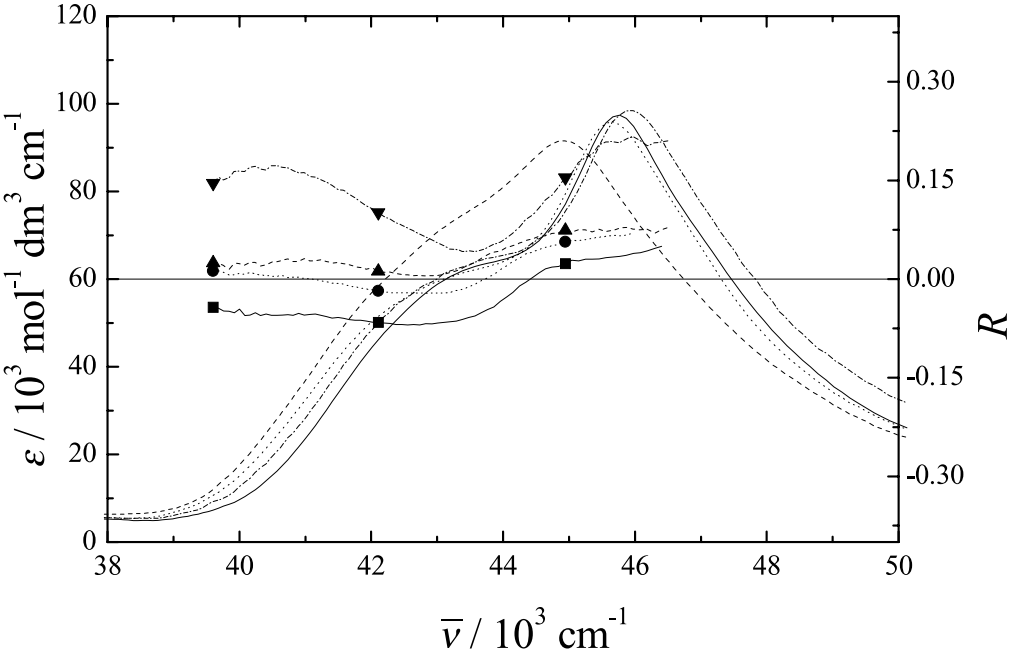

Fig. 6. The degree of anisotropy R of the bridged 1,1′-binaphthols (*R*)-**7** (—■—), (*R*)-**8** (- - - - -▲- - - - -), (*R*)-**9** (· · · · · ·●· · · · · ·), and (*R*)-**10** (-·-·▼-·-·) at $T = 28°C$ in ZLI-1695 and their UV spectra in the isotropic phase of ZLI-1695 at $T = 80°C$ ((*R*)-**7** (——), (*R*)-**8** (- - - - -), (*R*)-**9** (· · · · · ·), and (*R*)-**10** (-·-·-·))

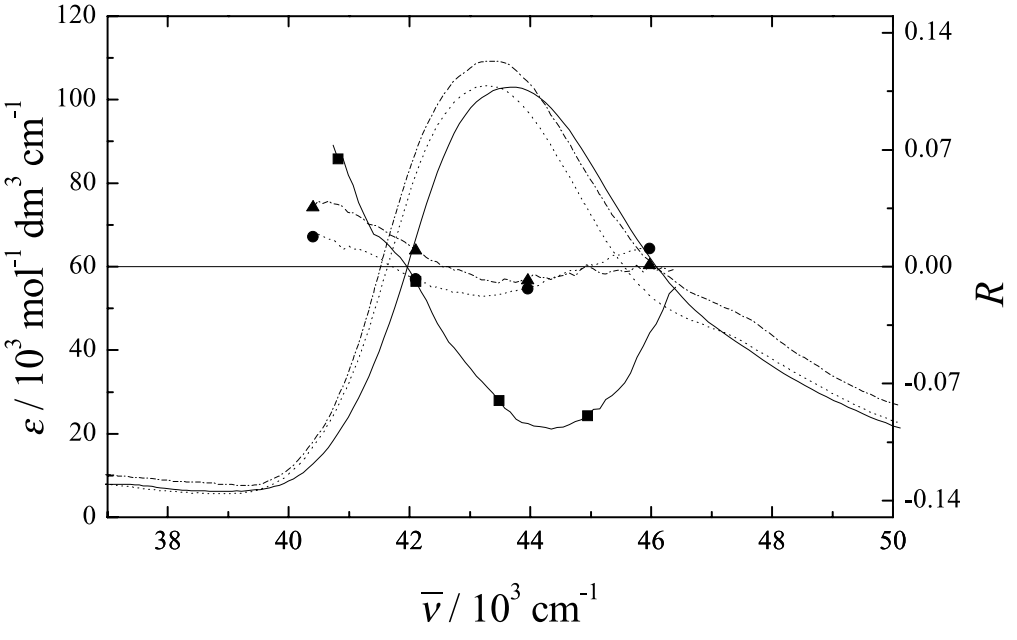

Fig. 7. The degree of anisotropy R of the unbridged 1,1′-binaphthols (*R*)-**4** (—■—), (*R*)-**5** (- - -●- - -), and (*R*)-**6** (-·-·▲-·-·) at $T = 28°C$ in ZLI-1695 and their UV spectra in the isotropic phase of ZLI-1695 at $T = 80°C$ ((*R*)-**4** (——), (*R*)-**5** (- - - - -), and (*R*)-**6** (-·-·-·))

both cases because the orientation axis lies for (*R*)-**8** parallel to the naphthyl–naphthyl bond and for (*R*)-**10** parallel to the C_2 symmetry axis. The long-wavelength exciton transition is of A→B symmetry and lies for (*R*)-**8** in the $x_1^*x_3^*$ plane and for (*R*)-**10** in the $x_1^*x_2^*$ plane. The interchange of the orientation of the orientation axis between (*R*)-**8** and (*R*)-**10** is further confirmed by the fact that *R* is of the same size in the short-wavelength band for (*R*)-**8** and in the long-wavelength band for (*R*)-**10**. With respect to the molecule's fixed coordinate system x_i, the not by symmetry fixed A→B transitions of (*R*)-**8** and (*R*)-**10** are approximately polarized in the same direction.

Negative *R* values can be obtained from transitions which are either polarized parallel to the x_1^* or the x_2^* direction.[f)] Thus, the long-wavelength bands of (*R*)-**7** and (*R*)-**9** can either be polarized in x_1^* or in x_2^* direction or in the $x_1^*x_3^*$ plane and their short-wavelength transitions in the x_2^*, the $x_1^*x_3^*$, or in the x_3^* direction. Therefore, one exciton transition of (*R*)-**7** and (*R*)-**9** has to be polarized in the $x_1^*x_3^*$ plane (A→B transition), the other one parallel to the C_2 symmetry axis – here the x_2^* axis (A→A transition). As pointed out above, a negative or positive degree of anisotropy is possible for both transitions. From the comparison of the size of the positive degree of anisotropy of (*R*)-**7** in the short-wavelength region with those of (*R*)-**8** and (*R*)-**9** in the long-wavelength region, a polarization parallel to the x_2^* axis for (*R*)-**7** and (*R*)-**9** can be suggested. Then the short-wavelength transition is of A→A symmetry. The A→B transition belongs to the negative degree of anisotropy. The latter conclusion for (*R*)-**7** and (*R*)-**9** has been derived from a qualitative comparison of *R* values. However, an unequivocal assignment can only be obtained by a quantitative calculation of *R* by Eqs. (15), (16), and (18) for which the order parameters have to be known.

The degree of anisotropy of the unbridged binaphthols (*R*)-**4** to (*R*)-**6** differs from that of the bridged binaphthol in its dispersion. There is a negative minimum approximately in the center of the absorption band. On the short wavelength side of the absorption band contributes a third transition to the band because *R* increase towards larger wave numbers for (*R*)-**4** to (*R*)-**6**. For (*R*)-**5** and (*R*)-**6** the *R* values are too small for a detailed analysis but the very weak shoulder on the short-wavelength side of the main absorption band, which is too far from the center of the main band to be an exciton transition, confirms the above postulated third transition. With this result the negative degree of anisotropy of (*R*)-**4** in the band center belongs to the short-wavelength exciton transition which is polarized either in x_1^* or in x_2^* direction. The ^{2}H NMR spectroscopy assigns the naphthyl–naphthyl bond to be the orientation axis [27]. Together with the results of the ^{2}H NMR spectroscopy [27] one may conclude for (*R*)-**4** that the A→A transition is polarized parallel to the x_1^* direction and the A→B transition is polarized in the $x_2^*x_3^*$ plane. Then, the A→B transition includes an angle different from zero with the orientation axis which leads to a small positive degree of anisotropy.

Summarizing the discussion of the degree of polarization, the long-wavelength transition of (*R*)-**4** to (*R*)-**10** belongs to an A→B (α band) and the short-wavelength

[f)] In principle, x_1^* have to have a negative degree of anisotropy whereas a x_2^* polarized transition can lead either to a positive or negative degree of anisotropy if and only if *Saupe*'s order parameter *D* is different from zero; $R > 0$ for all in x_3^* direction polarized transitions

transition to an A→A (β band) transition. The transition moment of the A→B transition includes a large angle between both principal axes of the order tensor in the plane perpendicular to the C_2 symmetry axis what follows from the relative small negative or positive values of the degree of anisotropy of (*R*)-**4** to (*R*)-**10** in the spectral region of the long-wavelength band. This angle can be evaluated quantitatively in context with the calculation of the tensor coordinates of the absorption tensor from the experimentally determined *R* as will be discussed later. Furthermore, the unbridged as well as the bridged binaphthols possess in the spectral region of the exciton bands a third transition not belonging to the exciton band system.

Binaphthols – CD Spectroscopy

The negative couplets of the bridged and unbridged 1,1′-binaphthols (*R*)-**4** to (*R*)-**10** are based on a long-wavelength A→B and a short-wavelength A→A transitions as shown above. According to the exciton chirality rule [7] the negative couplet of (*R*)-**4** to (*R*)-**10** belongs to a negative chirality of the conformers in solutions and crystals. The size of their amplitudes corresponds to the dihedral angles as determined by the X-ray analysis and the result of an AM1 calculation for the gaseous state [26]. The

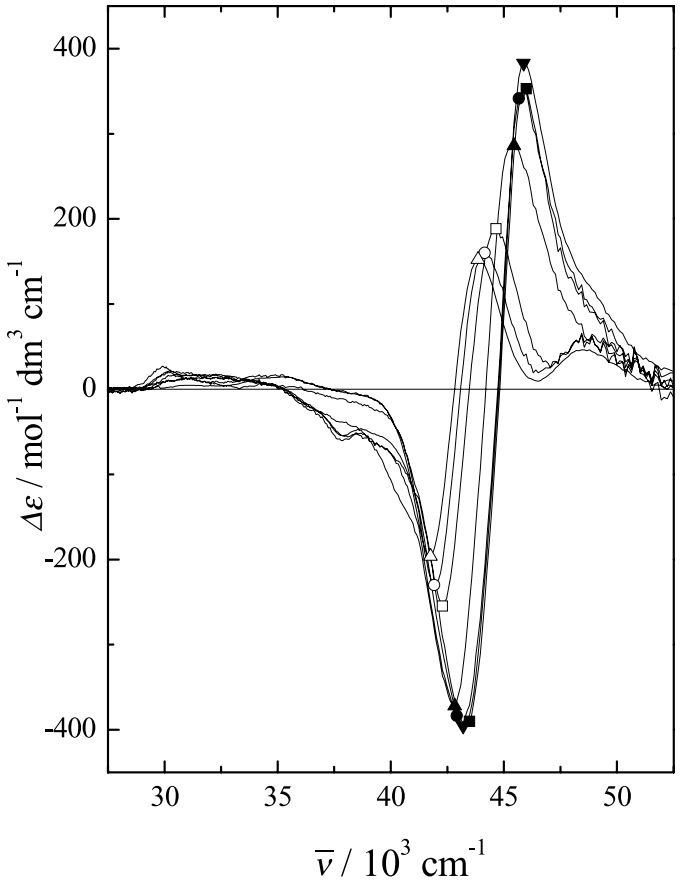

Fig. 8. Circular dichroism of (*R*)-**4** (□), (*R*)-**5** (○), (*R*)-**6** (△), (*R*)-**7** (■), (*R*)-**8** (▲), (*R*)-**9** (●), and (*R*)-**10** (▼) at $T = 80°C$ in the isotropic phase of ZLI-1695

amplitudes of the unbridged binaphthols (*R*)-**4** to (*R*)-**6** are smaller by a factor of about 1.8 than those of the bridged compounds. This decrease can be traced back on an extremely broad potential as a function of the dihedral angle about the naphthyl–naphthyl bond. The large amplitude motion LAM [28] within this potential allows a broad distribution of conformers possessing positive and negative couplets by which in the mean a decrease of the amplitude of the CD results [29]. This broad distribution of conformers is also responsible for the decrease and the change of the dispersion of the degree of anisotropy because the orientation of the principal axes of the order tensor as well as the size of the order parameter of the different conformers varies due to their very different length to breadth ratio.

The decrease of the mean amplitude of the CD and the variation of the dispersion of the degree of anisotropy in comparison with the properties of the bridged binaphthols have its analogous phenomenon in the chiral induction of cholesteric phases of the 1,1′-binaphtols. This analogy also proves the existence of a broad distribution of conformers with their broad orientational distribution function. Whereas the chiral induction of the bridged molecules leads to a large helical twisting power (*HTP*), the *HTP* of the unbridged binaphthols is about zero or even change sign ((*R*)-**6**, Fig. 9). This analogy can be traced back to a very similar

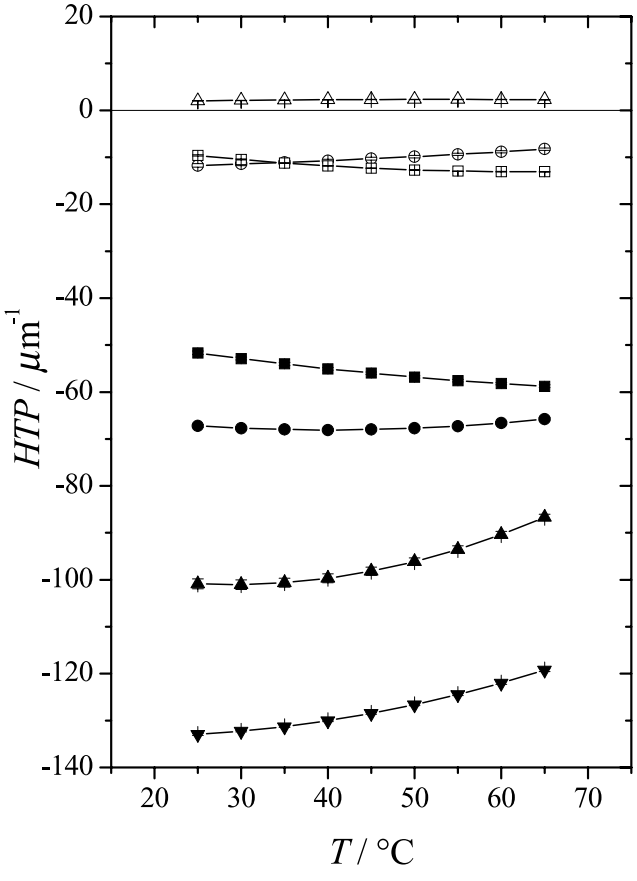

Fig. 9. Temperature dependence of the *HTP* of (*R*)-**4** (□), (*R*)-**5** (○), (*R*)-**6** (△), (*R*)-**7** (■), (*R*)-**8** (▲), (*R*)-**9** (●), and (*R*)-**10** (▼) in ZLI-1695

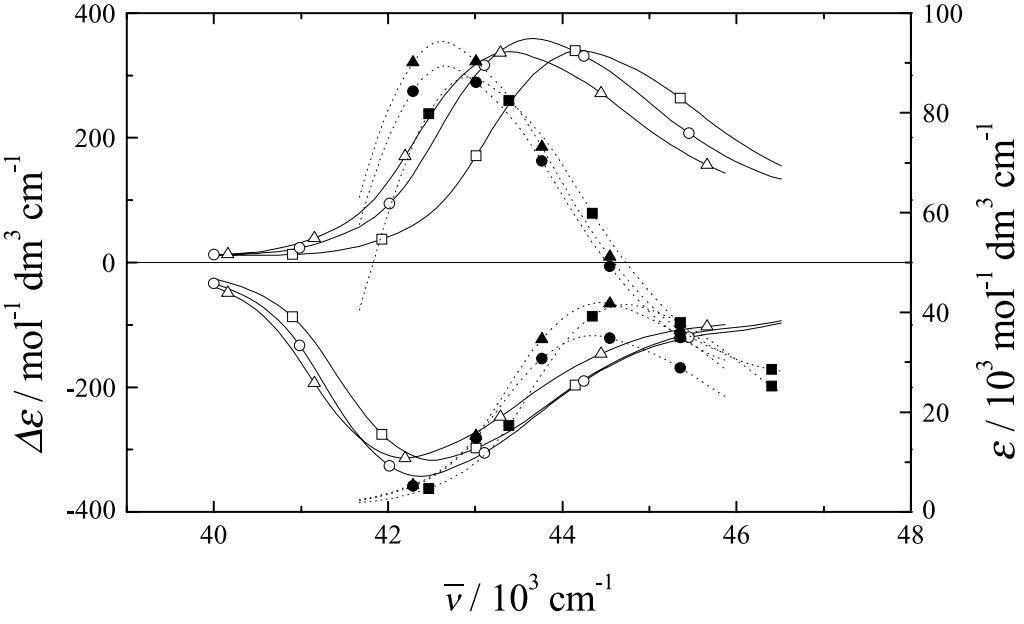

Fig. 10. The long-wavelength and short-wavelength exciton CD bands $\Delta\varepsilon^{\alpha}$ (A→B) and $\Delta\varepsilon^{\beta}$ (A→A) [(*R*)-**4** (□), (*R*)-**5** (○), and (*R*)-**6** (△)] and the long-wavelength and short-wavelength exciton UV bands ε^{α} (A → B) and ε^{β} (A → B) [(*R*)-**4** (■), (*R*)-**5** (●), and (*R*)-**6** (▲)] from the fit of the experimental CD and UV spectra in ZLI-1695 at $T = 80°C$

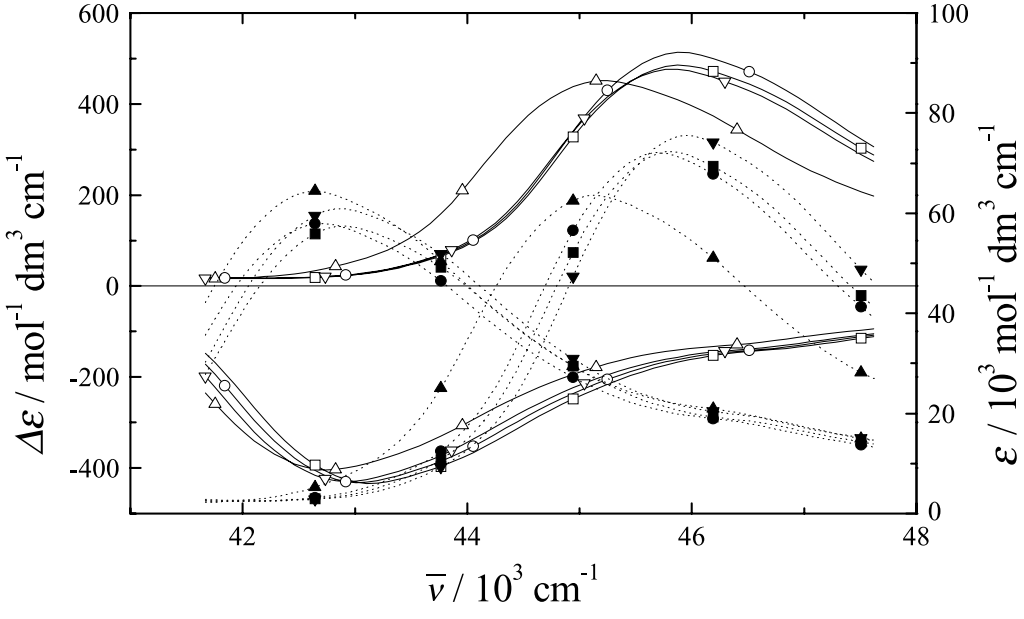

Fig. 11. The long-wavelength and short-wavelength exciton CD bands $\Delta\varepsilon^{\alpha}$ (A→B) and $\Delta\varepsilon^{\beta}$ (A→A) [(*R*)-**7** (□), (*R*)-**8** (△), (*R*)-**9** (○), and (*R*)-**10** (▽)] and the long-wavelength and short-wavelength exciton UV bands ε^{β} (A→B) and ε^{α} (A→B) [(*R*)-**7** (■), (*R*)-**8** (▲), (*R*)-**9** (●), and (*R*)-**10** (▼)] from the fit of the experimental CD and UV spectra in ZLI-1695 at $T = 80°C$

interaction model which leads to identical structures of the equations for the description of the degree of anisotropy (Eq. (18)), the anisotropy of the CD (ACD, Eq. (8)), and for the *HTP* [30] (Eq. (36)).

$$HTP = \sum_{i,j} g_{ij33} W_{ij} \tag{36}$$

The weighted mean of the chirality interaction tensor W_{ij} reduces the *HTP* of the unbridged 1,1′-binaphthols because of the very different length to breadth ratios of the different conformers which are decisive for the orientational distribution of the dissolved 1,1′-binaphthol, *i.e.*, the g^*_{ii33} are largely changed by the LAM.

To decompose the exciton couplets as well as the exciton UV bands of the binaphthols into the contributions of the α (A→B) and β (A→A) bands, these spectra have been fitted by an exciton model using the shape of the UV spectrum of 2-hydoxynaphthalene as a suitable spectral function (Figs. 10, 11). The fitting parameters are the angle between the transition moments of the subunits ϑ, the

Table 1. Spectroscopic data and structure parameters of the binaphthols (*R*)-**4** to (*R*)-**10**

	(*R*)-**4**	(*R*)-**5**	(*R*)-**6**	(*R*)-**7**	(*R*)-**8**	(*R*)-**9**	(*R*)-**10**
$\Delta\varepsilon_{min}/mol^{-1}\,dm^3\,cm^{-1}$ in ZLI-1695, $T = 80°C$	−255	−230	−196	−396	−394	−372	−396
$\overline{\nu}_{min}/cm^{-1}$ in ZLI-1695, $T = 80°C$	42283	41929	41754	43290	43103	42827	43197
$\Delta\varepsilon_{max}/mol^{-1}\,dm^3\,cm^{-1}$ in ZLI-1695, $T = 80°C$	188	160	153	353	350	286	383
$\overline{\nu}_{max}/cm^{-1}$ in ZLI-1695, $T = 80°C$	44643	44150	43860	45977	45767	45249	45872
$\varepsilon_{max}/10^3\,mol^{-1}\,dm^3\,cm^{-1}$ in ZLI-1695, $T = 80°C$	102.974	103.321	109.147	97.373	95.931	91.551	98.436
$\overline{\nu}_{max}/cm^{-1}$ in ZLI-1695, $T = 80°C$	43764	43290	43384	45767	45662	44944	45977
θ_{RSA}[a)]/°	−78.6[b)]/−89.5[c)]	−111.0[d)]	−70.6/−73.0[e)]	−59.8[f)]	−59.9[g)]	−64.4[h)]	−53.0[i)]
θ_{AM1}/°	−106.8[j)]	−87.0[j)]	−93.4[j)]	−52.8[j)]	−52.2[j)]	−60.1[j)]	−52.2[j)]
V_{ij}/cm^{-1}	335.9[k)]	94.0[k)]	0.0[k)]	1091.9[k)]	1044.6[k)]	–	1144.2[k)]
$\Delta\bar{\nu}_s/cm^{-1}$	50.5[k)]	−379.7[k)]	−285.4[k)]	806.5[k)]	853.8[k)]	–	905.8[k)]
V_{ij}/cm^{-1}	848.3[l)]	647.1[l)]	603.2[l)]	1376.8[l)]	1448.5[l)]	1232.4[l)]	1435.7[l)]
$\Delta\bar{\nu}_s/cm^{-1}$	−441.3[l)]	−788.6[l)]	−1015.2[l)]	709.7[l)]	576.1[l)]	180.8[l)]	666.8[l)]
$R^{\alpha}_f/10^{-38}$ cgs	−7.37[l)]	−7.76[l)]	−7.90[l)]	−9.90[l)]	−9.85[l)]	−9.34[l)]	−10.70[l)]
ϑ/° aus CD in ZLI-1695	89.1[l)]	89.5[l)]	88.7[l)]	88.6[l)]	88.9[l)]	88.4[l)]	86.9[l)]
ϑ/° aus UV in ZLI-1695	111.8[m)]	116.7[m)]	113.7[m)]	85.3[m)]	85.7[m)]	92.0[m)]	85.8[m)]
$\frac{D^{NK}_{1,1'\text{-binaphthol}}}{D^{NK}}$	1.98[n)]	2.11[n)]	2.12[n)]	2.07[n)]	2.08[n)]	2.12[n)]	2.08[n)]

[a)] θ is the dihedral angle between unit vectors perpendicularly oriented to the naphthyl-planes in the mean of (*R*)-**4** to (*R*)-**10** from X-ray [38] and AM1 calculations [26]; [b)] *R* enantiomer ((*R*)-**1**) [36]; [c)] racemic crystal ((*R*/*S*)-**1**) [36]; [d)] racemic crystal ((*R*/*S*)-**2**) [37]; [e)] racemic crystal ((*R*/*S*)-**3**), two crystallographic independent molecules in the unit cell [38]; [f)] racemic crystal ((*R*/*S*)-**4**) [38]; [g)] racemic crystal ((*R*/*S*)-**5**) [38]; [h)] *R* enantiomer ((*R*)-**6**) [38]; [i)] racemic crystal ((*R*/*S*)-**7**) [38]; [j)] calculated by the AM1 method [26]; [k)] decomposition into the tensor coordinates taking the degree of anisotropy [26] and the order S^* and D^* determined by ^{2}H NMR into account [27]; [l)] fit of the experimental CD spectra in ZLI-1695 by use of the exciton theory [26]; [m)] fit of the experimental UV spectra in ZLI-1695 by use of the exciton theory [26]; [n)] ratio of the dipole strengths of the 1,1′-binaphthols **1** to **7**, $D^{NK}_{1,1'\text{-binaphthol}}$, and the dipole strength D^{NK} of 2-hydroxynaphthalene

Davydov split V_{ij}, the rotational strength of the exciton bands $R_f^{\alpha} = -R_f^{\beta}$ (Table 1), the variation of the ratio of the dipole strength of the subunit and the dipole strength of the exciton band, and in addition a mean shift of the position of the absorption band of the subunit 2-hydoxynaphthalene $\bar{\nu}_s$. The fitting parameter from the UV and the CD bands are consistent. A higher quality of the fitting is obtained from the CD because the bands of both transitions are of different sign (Table 1). The *Davydov* split of the unbridged compounds is smaller than the split of bridged 1,1′-binaphthols. The CD as well the UV intensity of the α and β band (A→B and A→A transition) are of equal size for the unbridged compounds whereas for the bridged compounds the A→B transition contributes with about 70–80% of the intensity of the A→A transition to the total intensity as expected for the different dihedral angles found for the bridged and unbridged compounds. The angles between the transition moment directions of the subunits ϑ found for the UV and CD are somewhat different but acceptable within the experimental error.

Binaphthols – Polarized Spectroscopy

For an independent proof of the decomposition of the isotropic UV spectra, the diagonal elements of the tensor of absorption ε_{ii}^{*} have been evaluated from the degree of anisotropy, the order tensor (g_{ii33}^{*}; i = 1, 2, 3), and the absorption $\varepsilon(\bar{\nu})$ (Figs. 6, 7). The absorption coefficient ε^{α} (A→B) is for (*R*)-**10** a sum of two tensor coordinates ε_{11}^{*} and ε_{22}^{*} whereas ε^{β} (A→A) is determined by the tensor coordinates ε_{33}^{*} (Figs. 12, 13). The *Davydov* splits are larger than those obtained from the fitting of the isotropic

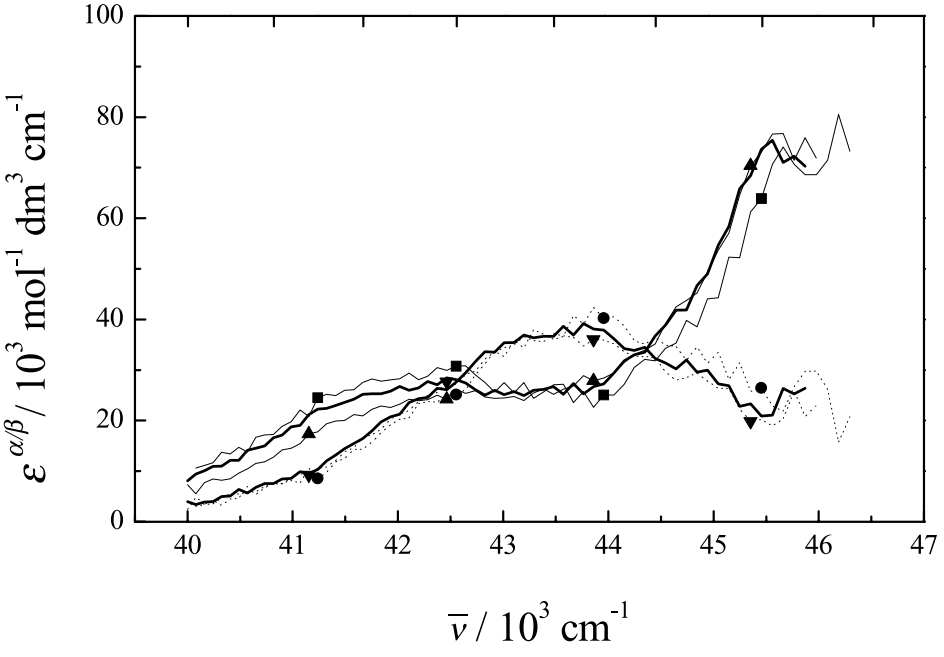

Fig. 12. The absorption spectrum of the α (A→B) transition $\varepsilon^{\alpha} = \left(\varepsilon_{11}^{*\alpha} + \varepsilon_{22}^{*\alpha}\right)/3$ [(*R*)-**7** (▲), (*R*)-**9** (—), and (*R*)-**10** (■)] and of the β (A→B) transition $\varepsilon^{\beta} = \varepsilon_{33}^{*\beta}/3$ [(*R*)-**7** (▼), (*R*)-**9** (—), and (*R*)-**10** (●)] of the bridged binaphthols calculated from the degree of anisotropy, the order tensor, and the UV absorption bands

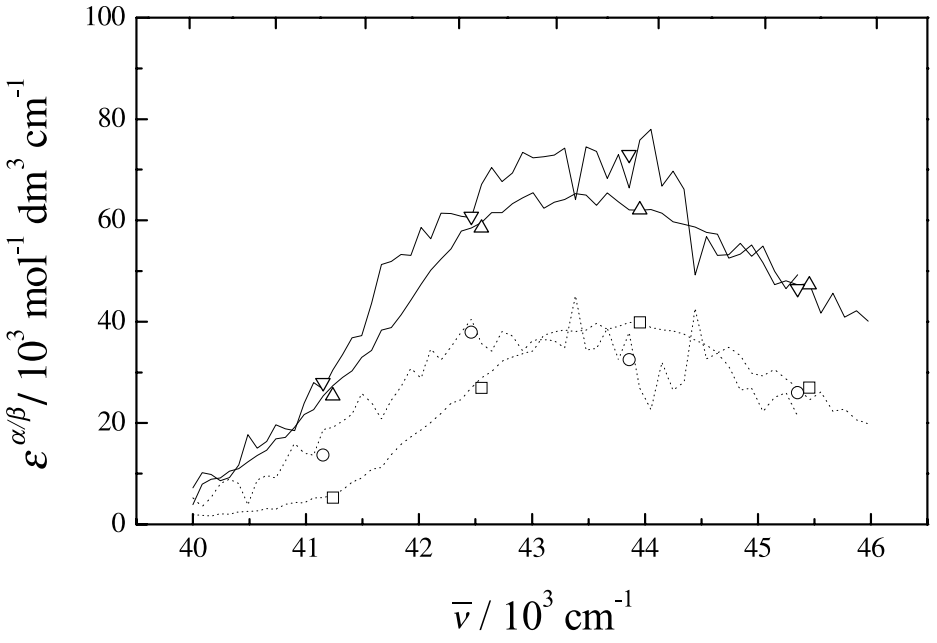

Fig. 13. The absorption spectrum of the α (A→B) transition $\varepsilon^{\alpha} = \left(\varepsilon_{11}^{*\alpha} + \varepsilon_{22}^{*\alpha}\right)/3$ [(*R*)-**4** (Δ), and (*R*)-**6** (▽)] and of the β (A→B) transition $\varepsilon^{\beta} = \varepsilon_{33}^{*\beta}/3$ [(*R*)-**4** (□), and (*R*)-**6** (○)] of the unbridged binaphthols calculated from the degree of anisotropy, the order tensor, and the UV absorption bands; for (*R*)-**5** no order parameters are available because of its small solubility in ZLI-1695

spectra (Table 1) but consistent within the experimental error. The total intensities also correspond to the results obtained from the isotropic spectra as depicted in Figs. 10 and 11. The quotient of the two coordinates $\varepsilon_{11}^{*}/\varepsilon_{22}^{*}$ of the A→B transition yields the angle of the transition moment direction with respect to the coordinate axes x_1^{*} in the plane perpendicular to the C_2 symmetry axis. For (*R*)-**10** and similarly for all other binaphtholes of Scheme 3 the angle is about 50° which means that the transition moment and the naphthyl–naphthyl bond include an angle of about 50° [26].

Finally, there is an unexpected result for (*R*)-**7** to (*R*)-**10**. At the long wavelength side of the β band a third band appears, overlapping ε^{α} (A→B), which is polarized parallel to the β band (Fig. 12). One may assume that the strong interaction of both binaphthols leads to an additional transition polarized parallel to the C_2 symmetry axis which is of unknown origin. This band falsifies the decomposition of the isotropic UV and CD spectra because the intensity of the additional band is counted there for the α band. Theoretical calculations of the spectra are needed for an assignment of this third transition.

The results for the unbridged binaphthols are affected, as for the decomposition of the isotropic spectra, by the small *Davydov* split and their structureless UV band. In spite of that, the analysis of (*R*)-**4** and (*R*)-**6**, shown in Fig. 13, allows a comparison for the decomposition of the CD and UV spectra (Figs. 10) which are consistent. The angle between the naphthyl–naphthyl bond and the A→B transition moment direction is in the same order of magnitude as for the bridged compounds. There is also a third absorption band of unknown origin as discussed before. But this band is in contrast to that of the bridged compounds positioned at the short wavelength side of the exciton band system.

Binaphthols – ACD Spectra

The $\Delta\varepsilon^{A}$ spectra of the exciton transitions of the binaphthols (*R*)-**4** to (*R*)-**10** maintain their couplet shapes as a function of temperature as shown for (*R*)-**4**[g] (Fig. 14). Their amplitudes $|\Delta\varepsilon^{A}|$ decreases with increasing temperature (Figs. 15–17). Except for (*R*)-**10** the bisigmoidal shape of $\Delta\varepsilon^{A}(\bar{\nu}) - \Delta\varepsilon(\bar{\nu})$ is symmetric for all temperatures as depicted for (*R*)-**4** and (*R*)-**9** in Figs. 15 and 16. The asymmetric increase of the negative lobe of (*R*)-**10** is a hint for an asymmetric orientation of the exciton transition moments in the oriented ensemble of molecules with respect to the propagation direction of light (Fig. 17). These findings resemble a phenomenon discussed above for the dibenzoate (*S*)-**1** where the positive lobes of the couplet disappear with increasing temperature (Fig. 3).

The coordinates of the UV and CD tensor of (*R*)-**9** and (*R*)-**10** are equal within the experimental error if given with respect to the same principal axes of the order tensor (Figs. 6, 8). The CD tensor coordinate of (*R*)-**10** belonging to the direction of the C_2 symmetry axis is small, *i.e.*, in a rough approximation about zero[h] ($\Delta\varepsilon^{*}_{33}$ if the x^{*}_{3} axis is chosen for the C_2 axis). A large negative couplet has been observed with a light beam propagating along the naphthyl–naphthyl bond ($\Delta\varepsilon^{*}_{22}$). With light propagating perpendicular to this bond and perpendicular to the C_2 symmetry axis ($\Delta\varepsilon^{*}_{11}$) a positive couplet has been obtained (Fig. 18).

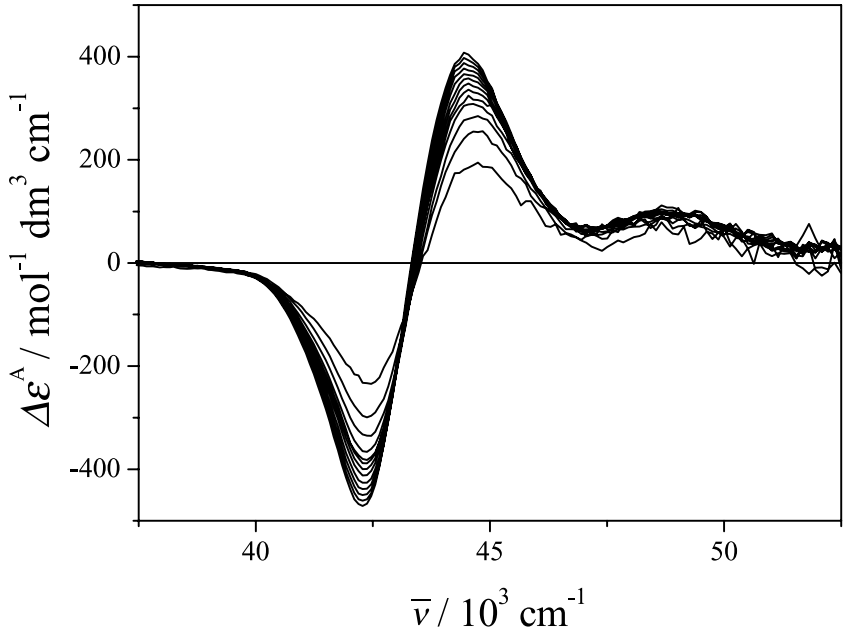

Fig. 14. The ACD ($\Delta\varepsilon^{A}$) of (*R*)-**4** in ZLI-1695 for the reduced temperatures T^{*} ($=T/T_n$) and the CD ($\Delta\varepsilon$) ordered from below for the negative lobe or from above for the positive lobe: 0.88, 0.89, 0.90, 0.91, 0.92, 0.93, 0.94, 0.95, 0.96, 0.97, 0.98, 0.99; $T = 80$°C (iso); T_n is the temperature of the phase transition nematic/isotropic

[g] The ACD spectra of (*R*)-**9** and (*R*)-**10** are published in Ref. [10]

[h] It should be brought to remembrance that the molecular ensemble with which the ACD is measured has to possess a rotationally symmetric distribution about the propagation direction of the light beam

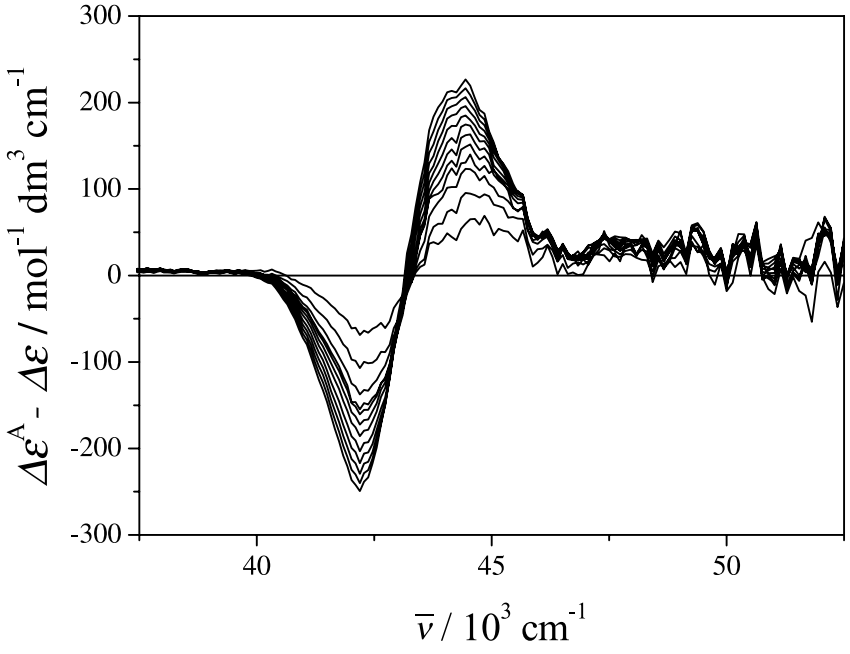

Fig. 15. The difference $\Delta\varepsilon^A - \Delta\varepsilon$ of (*R*)-**4** in ZLI-1695 for the reduced temperatures T^* ordered from below for the negative lobe or from above for the positive lobe: 0.88, 0.89, 0.90, 0.91, 0.92, 0.93, 0.94, 0.95, 0.96, 0.97, 0.98, 0.99

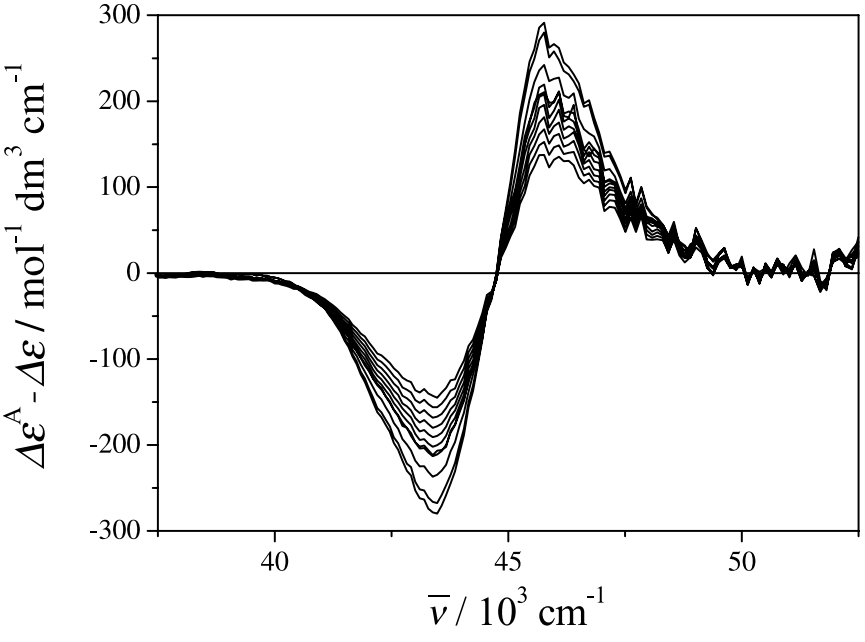

Fig. 16. The difference $\Delta\varepsilon^A - \Delta\varepsilon$ of (*R*)-**9** in ZLI-1695 for the reduced temperatures T^* ordered from below for the negative lobe or from above for the positive lobe: 0.89, 0.90, 0.91, 0.92, 0.93, 0.94, 0.95, 0.96, 0.97, 0.98, 0.99

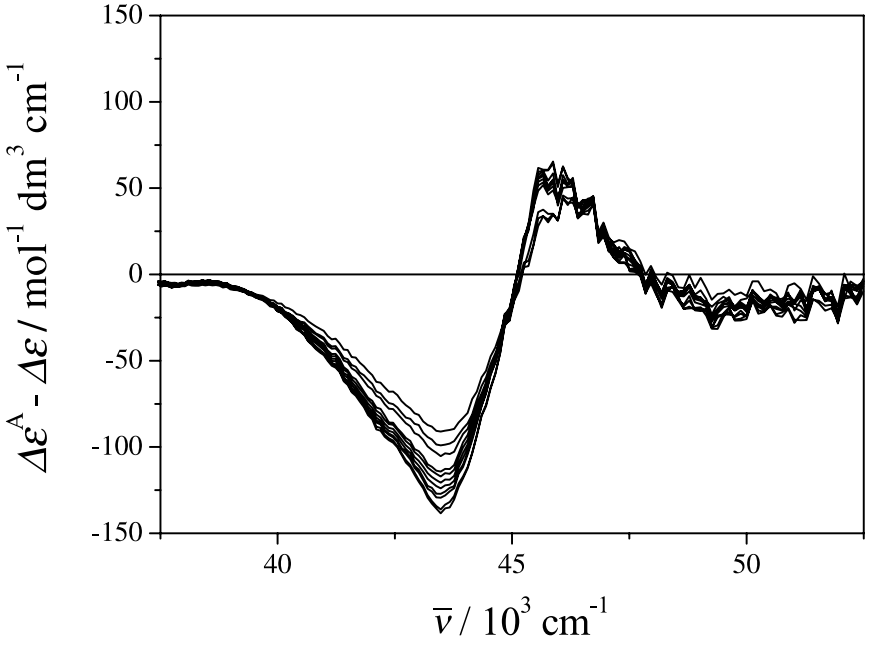

Fig. 17. The difference $\Delta\varepsilon^A - \Delta\varepsilon$ of (*R*)-**10** in ZLI-1695 for the reduced temperatures T^* ordered from below for the negative lobe or from above for the positive lobe: 0.89, 0.90, 0.91, 0.92, 0.93, 0.94, 0.95, 0.96, 0.97, 0.98, 0.99

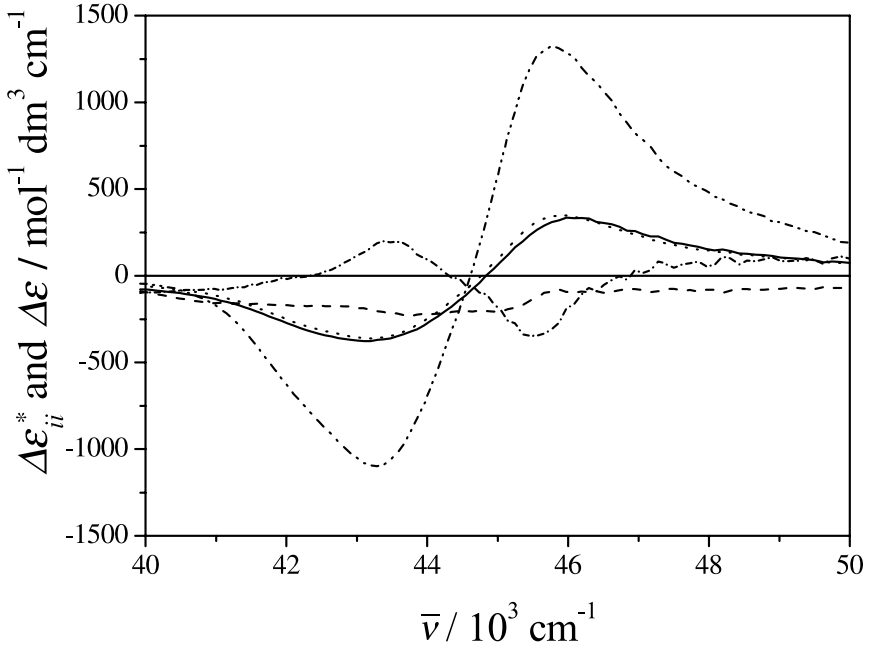

Fig. 18. The tensor coordinates $\Delta\varepsilon^*_{11}$ (-·····), $\Delta\varepsilon^*_{22}$ (-·-·-·-·-), and $\Delta\varepsilon^*_{33}$ (- - - - -), the CD $\Delta\varepsilon$ (—) and the recalculated CD $\Delta\varepsilon_{calc}$ (· · · · · ·) of (*R*)-**9** and (*R*)-**10** in ZLI-1695 given with respect to the principal axis of the order tensor of (*R*)-**10**

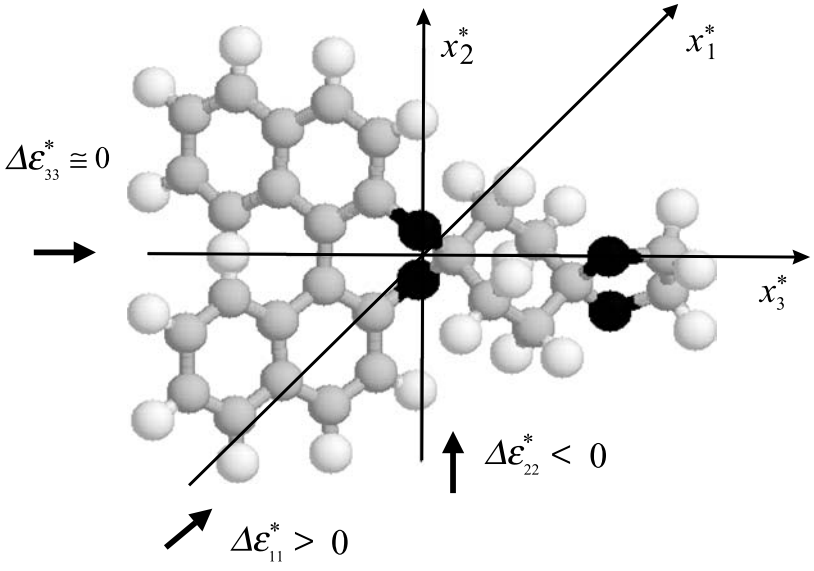

Fig. 19. The geometry according to an AM1 calculation for (*R*)-**10** [26]; the distinct right- and left-handed helical structure can be recognized along the x_2^* and x_1^* direction for which also a CD couplet of different sign has been obtained, respectively ($\Delta\varepsilon_{22}^* < 0$, $\Delta\varepsilon_{11}^* > 0$ at about 45000 cm^{-1})

According to *Snatzke* [31] compounds of C_2 symmetry like the binaphthols possess along these two directions a right-handed and a left-handed helical structure, respectively. This handedness along both directions comes into being by a dihedral angle about the naphthyl–naphthyl bond different from zero (Table 1). As depicted in Fig. 8 this different handedness leads to CD couplets of different sign. Whereas the left-handed helical structure along the x_1^* axis of the (*R*)-configured binaphthol leads to a positive couplet, the right-handed helical structure along the x_2^* direction yields a negative couplet (Fig. 19). Even a correlation to the slope of these helices seems to exist: the larger elongation of the helix with the larger pitch along the naphthyl–naphthyl bond yields the larger CD ($|\Delta\varepsilon_{22}^*| > |\Delta\varepsilon_{33}^*|$). The same argumentation holds for (*R*)-**9** except that the numbering of the tensor coordinates has to be interchanged because they refer to its own principal axes of the order tensor which are differently oriented in the skeletons of (*R*)-**9** and (*R*)-**10**: $\Delta\varepsilon_{33}^*$ ((*R*)-**9**)$\rightarrow\Delta\varepsilon_{22}^*$ ((*R*)-**10**) and $\Delta\varepsilon_{22}^*$ ((*R*)-**10**)$\rightarrow\Delta\varepsilon_{33}^*$ ((*R*)-**9**). For (*R*)-**8** the same result is obtained except that the amplitude of $\Delta\varepsilon_{33}^*$ is smaller than the amplitude of (*R*)-**9** or (*R*)-**10** (Table 1).

For unbridged binaphthols the tensor coordinate measured along the naphthyl–naphthyl bond is the only one which contributes essentially to the total CD effect (Fig. 14). Their couplet shapes are similar to those of the bridged compounds (Fig. 18). The amplitudes of the CD couplets (Fig. 8) are smaller about a factor 3 to 4. This fits to the stronger overlap and, thus a larger canceling of both exciton bands because of their smaller *Davydov* split. But, in addition, the dihedral angle about 110° together with the LAM about the naphthyl–naphthyl bond also reduce their amplitude of the couplet [29].

In the preceding sections always the tensor coordinates $\Delta\varepsilon_{ii}^*$ have been analyzed. They depend on the components of the corresponding transition moments in the plane of the molecule perpendicular to the propagation direction of light beams used for their

measurements (Eqs. (33)–(35)). One may ask also for the contribution of the components of the transition moments along a chosen direction within the molecule to the CD spectrum which can be obtained by linear combinations of the CD tensor coordinates as follows (Eqs. (37)–(39)).

$$\Delta_1(\bar{\nu}) = \frac{1}{2}(\Delta\varepsilon_{11} - \Delta\varepsilon_{22} - \Delta\varepsilon_{33}) = \frac{1}{2}B\bar{\nu}\sum_{\mathrm{n}} \mathrm{i}\langle\mu_1\rangle_{0\mathrm{n}}\langle m_1\rangle_{\mathrm{n}0}G^{0\mathrm{n}}(\bar{\nu}) + \Delta\varepsilon_{11}^{\mu\mathrm{Q}} \quad (37)$$

$$\Delta_2(\bar{\nu}) = \frac{1}{2}(\Delta\varepsilon_{22} - \Delta\varepsilon_{11} - \Delta\varepsilon_{33}) = \frac{1}{2}B\bar{\nu}\sum_{\mathrm{n}} \mathrm{i}\langle\mu_2\rangle_{0\mathrm{n}}\langle m_2\rangle_{\mathrm{n}0}G^{0\mathrm{n}}(\bar{\nu}) + \Delta\varepsilon_{22}^{\mu\mathrm{Q}} \quad (38)$$

$$\Delta_3(\bar{\nu}) = \frac{1}{2}(\Delta\varepsilon_{33} - \Delta\varepsilon_{11} - \Delta\varepsilon_{22}) = \frac{1}{2}B\bar{\nu}\sum_{\mathrm{n}} \mathrm{i}\langle\mu_3\rangle_{0\mathrm{n}}\langle m_3\rangle_{\mathrm{n}0}G^{0\mathrm{n}}(\bar{\nu}) + \Delta\varepsilon_{33}^{\mu\mathrm{Q}}$$

$$= -\frac{3}{2}\Delta\varepsilon - \Delta_1 - \Delta_2 \quad (39)$$

$\Delta\varepsilon_{ii}^{\mu\mathrm{Q}}$ ($i = 1, 2, 3$) is the electric dipole/electric quadrupole contribution to the CD (Appendix A.5: Eqs. (A-7)–(A-9)). Because of the C_2 symmetry of the binaphthols of Scheme 3, two special cases are of importance for the Δ_is:

Case 1

1) The orientation axis lies parallel to the C_2 symmetry axis; 2) the A→A (0→1) transition is polarized parallel to the x_3^* axis. The electric dipole transition moment given by its coordinates with respect to the principal axes of the order tensor is $\langle\mu_1^*\rangle_{01} = \langle\mu_2^*\rangle_{01} = 0$, $\langle\mu_3^*\rangle_{01} \neq 0$. The band shape is given by $G^{01}(\bar{\nu})$; 3) the A→B (0→2) transition is polarized in the $x_1^*x_2^*$ plane. The electric dipole transition moment given by its coordinates with respect to the principal axes of the order tensor is $\langle\mu_1^*\rangle_{02} \neq 0$, $\langle\mu_2^*\rangle_{02} \neq 0$, $\langle\mu_3^*\rangle_{02} = 0$. The band shape is given by $G^{02}(\bar{\nu})$.

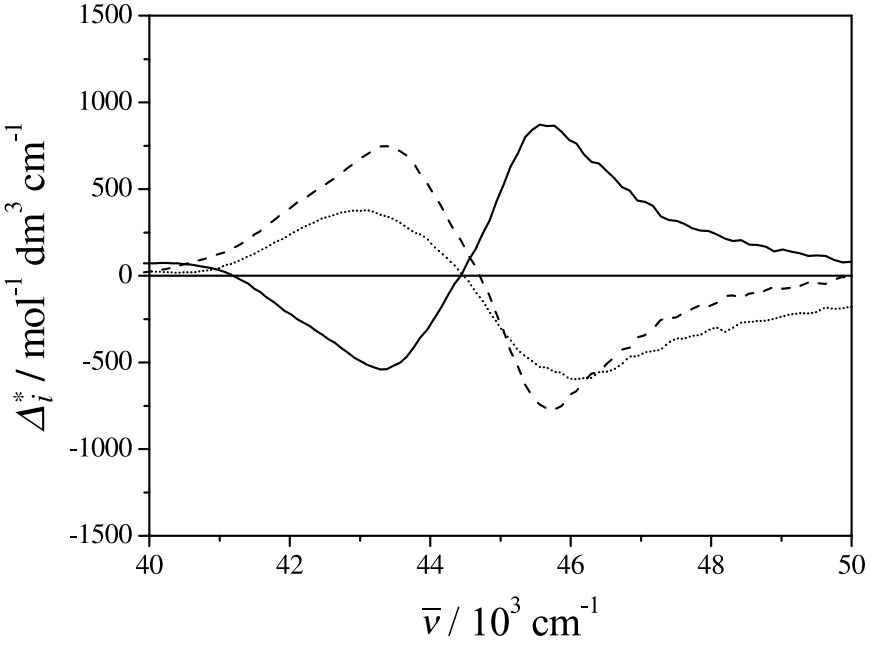

Fig. 20. Δ_1^* (—), Δ_2^* (- - - - -), and Δ_3^* (· · · · · ·) for (*R*)-**9** and (*R*)-**10** given with respect to the principal axes of the order tensor of (*R*)-**10** in ZLI-1695

Case 2

1) The orientation axis lies in the plane perpendicular to the C_2 symmetry axis; 2) the A→A (0→1) transition is polarized parallel to the x_2^* axis or to the x_1^* axis. The electric dipole transition moment given by its coordinates with respect to the principal axes of the order tensor is $\langle\mu_1^*\rangle_{01} = 0$, $\langle\mu_2^*\rangle_{01} \neq 0$, $\langle\mu_3^*\rangle_{01} = 0$ or $\langle\mu_1^*\rangle_{01} \neq 0$, $\langle\mu_2^*\rangle_{01} = 0$, $\langle\mu_3^*\rangle_{01} = 0$. The band shape is given by $G^{01}(\bar{\nu})$; 3) the A→B (0→2) transition is polarized in the $x_1^*x_3^*$ or $x_2^*x_3^*$ plane. The electric dipole transition moment given by its coordinates with respect to the principal axes of the order tensor is $\langle\mu_1^*\rangle_{02} \neq 0$, $\langle\mu_2^*\rangle_{02} = 0$, $\langle\mu_3^*\rangle_{02} \neq 0$ or $\langle\mu_1^*\rangle_{01} = 0$, $\langle\mu_2^*\rangle_{01} \neq 0$, $\langle\mu_3^*\rangle_{02} \neq 0$. The band shape is given by $G^{02}(\bar{\nu})$.

To analyze the experimental results of (*R*)-**10** (Fig. 20) Eqs. (37)–(39) have to be specialized for Case 1. Furthermore, the third transition polarized in the x_3^* direction has to be taken into account (Eqs. (40)–(42)).

$$\begin{aligned}\Delta_1^* &= \frac{1}{2}(\Delta\varepsilon_{11}^* - \Delta\varepsilon_{22}^* - \Delta\varepsilon_{33}^*)\\ &= \frac{1}{2}B\bar{\nu}\Bigg(\frac{\omega_{10}}{c}(\langle\mu_3^*\rangle_{01}\langle Q_{21}^*\rangle_{10})G^{01}(\bar{\nu})\\ &\quad + \left[\mathrm{i}\langle\mu_1^*\rangle_{02}\langle m_1^*\rangle_{20} - \frac{\omega_{20}}{c}\langle\mu_2^*\rangle_{02}\langle Q_{31}^*\rangle_{20}\right]G^{02}(\bar{\nu}) + \frac{\omega_{30}}{c}\langle\mu_3^*\rangle_{03}\langle Q_{21}^*\rangle_{30}G^{03}(\bar{\nu})\Bigg)\end{aligned} \tag{40}$$

$$\begin{aligned}\Delta_2^* &= \frac{1}{2}(\Delta\varepsilon_{22}^* - \Delta\varepsilon_{11}^* - \Delta\varepsilon_{33}^*)\\ &= \frac{1}{2}B\bar{\nu}\Bigg\{-\frac{\omega_{10}}{c}\langle\mu_3^*\rangle_{01}\langle Q_{12}^*\rangle_{10}G^{01}(\bar{\nu})\\ &\quad + \left(\mathrm{i}\langle\mu_2^*\rangle_{02}\langle m_2^*\rangle_{20} + \frac{\omega_{20}}{c}\langle\mu_1^*\rangle_{02}\langle Q_{23}^*\rangle_{20}\right)G^{02}(\bar{\nu}) - \frac{\omega_{30}}{c}\langle\mu_3^*\rangle_{03}\langle Q_{12}^*\rangle_{30}G^{03}(\bar{\nu})\Bigg\}\end{aligned} \tag{41}$$

$$\begin{aligned}\Delta_3^* &= \frac{1}{2}(\Delta\varepsilon_{33}^* - \Delta\varepsilon_{11}^* - \Delta\varepsilon_{22}^*)\\ &= \frac{1}{2}B\bar{\nu}\Bigg\{\mathrm{i}\langle\mu_3^*\rangle_{01}\langle m_3^*\rangle_{10}G^{01}(\bar{\nu}) + \frac{\omega_{20}}{c}(-\langle\mu_1^*\rangle_{02}\langle Q_{23}^*\rangle_{20} + \langle\mu_2^*\rangle_{02}\langle Q_{13}^*\rangle_{20})G^{02}(\bar{\nu})\\ &\qquad + \mathrm{i}\langle\mu_3^*\rangle_{03}\langle m_3^*\rangle_{30}G^{03}(\bar{\nu})\Bigg\}\end{aligned} \tag{42}$$

$G^{03}(\bar{\nu})$ is the band shape of the not assigned third transition. According to Eqs. (40)–(42) only one term in Δ_i $(i = 1, 2, 3)$ with either the band shape $G^{01}(\bar{\nu})$ or $G^{02}(\bar{\nu})$ is different from zero if all electric dipole/electric quadrupole contributions of the two exciton bands and of the third transition can be neglected. Then Δ_1^* and Δ_2^* are determined by the A→B transition with its band shape $G^{02}(\bar{\nu})$ and Δ_3^* is determined by the A→A transition with its band shape $G^{01}(\bar{\nu})$. *I.e.*, for an exciton system with two transitions without an electric dipole/electric quadrupole transition only one simple band has to be expected for each Δ_i^*. In contrast to this prediction for all Δ_i^* of (*R*)-**10** and also of (*R*)-**9** couplets have been observed, *i.e.*, the Δ_i^*s are determined at least by two or by three different dispersion functions, namely $G^{01}(\bar{\nu})$,

$G^{02}(\bar{\nu})$, and $G^{03}(\bar{\nu})$. Because $G^{03}(\bar{\nu}) \cong G^{02}(\bar{\nu})$ the third transition and the long-wavelength exciton transition is positioned in the same spectral region and thus, indistinguishable from the corresponding electric dipole/electric quadrupole contribution of the exciton A→B band. The long-wavelength lobe of Δ_3 is determined by the electric dipole/electric quadrupole contribution $-\langle\mu_1^*\rangle_{02}\langle Q_{23}^*\rangle_{20} + \langle\mu_2^*\rangle_{02}\langle Q_{13}^*\rangle_{20}$ and the electric dipole/magnetic dipole contribution $\mathrm{i}\langle\mu_3^*\rangle_{03}\langle m_3^*\rangle_{30}$ of the third transition. The short-wavelength lobes of Δ_1^* and Δ_2^* are determined by the electric dipole/electric quadrupole term $\langle\mu_3^*\rangle_{01}\langle Q_{12}^*\rangle_{10}$ which contributes with different signs to Δ_1^* and Δ_2^*. This theoretical prediction is proven experimentally: the positive and negative short-wavelength lobes of Δ_1 and Δ_2 are equal in their height (Fig. 20). Thus, these electric dipole/electric quadrupole contributions can be measured independently of a chosen origin of the coordinate system in spite of the fact that the information stems from an allowed electric dipole transition. The conditions under which such a contribution can be measured independently have been discussed in an earlier paper [14, 32]. The short-wavelength negative lobe of Δ_3 equals three times the negative CD of the A→A transition which is fulfilled within the experimental error.

Experimental

Highly ordered molecules are needed for the determination of anisotropic chiral effects, because these effects are often very small. Furthermore, these effects are often obscured by the anisotropy of achiral properties of the molecules. Therefore, the advantages of symmetry conditions have to be taken into account in order to avoid artifacts by an elliptical birefringence and elliptical dichroism which carry chirality information only in part. The ideal condition for chirality measurements of chiral anisotropic phases are uniaxial phases with which the ACD can be measured with a light beam propagating along the optical axis. This kind of measurements can be performed with every commercial CD instrument.

Liquid crystals (LC) are very powerful anisotropic solvents to orient dissolved guest molecules. The nematic phase ZLI-1695 (Merck), a mixture of four 4-alkyl-4′-carbonitrilbicyclohexanes with $R = C_2H_5$, C_3H_7, and C_7H_{15} with a nematic phase existing between 13–72°C, absorbs light only below 220 nm. If not explicitly mentioned, ZLI-1695 has been used for all presented measurements. Dissolved in an achiral nematic phases ZLI-1695, *e.g.*, chiral compounds of sufficient form anisotropy can be ordered to an amount of 50 to 60% but they also induce suprastructural chirality, *i.e.*, a helical structure with a pitch p (chiral nematic phase N*, cholesteric phase). The pitch p exerted by the dopant in a chiral nematic N* (cholesteric) phase is a measure for the force of the induction of a helical structure which is quantitatively described by the Helical Twisting Power (*HTP*). For a phase consisting of a chiral host and a chiral guest the *HTP* is defined by Eq. (43) with x_e and x_{e*} being the mole fractions of the enantiomers e and e*. For an achiral host phase Eq. (44) is valid and for small mole fractions x_e Eq. (45) is obtained.

$$(HTP)_e = \frac{1}{2}\left\{\left(\frac{\partial p^{-1}}{\partial x_e}\right)_{x_e=0} - \left(\frac{\partial p^{-1}}{\partial x_{e*}}\right)_{x_{e*}=0}\right\} \tag{43}$$

$$\left(\frac{\partial p^{-1}}{\partial x_e}\right)_{x_e=0} = -\left(\frac{\partial p^{-1}}{\partial x_{e*}}\right)_{x_{e*}=0} \tag{44}$$

$$(HTP)_e = \frac{1}{p x_e} \tag{45}$$

The CD and ORD of a chiral nematic phase N* (cholesteric phase) is mainly a phase and not a molecular property because even a very, very small guest concentration induces in cholesteric phases a significant pitch. Therefore, one has to unwind the helical pitch of the phase very carefully, *e.g.*, with a strong electric field, before the ACD measurement can be performed. Otherwise the molecular CD

effect can be falsified by contributions of the CD of the suprastructural chirality of the phase which outweighs the molecular effects by orders of magnitude. In an uncoiled cholesteric phase, the very strong temperature dependence of $\Delta\varepsilon^{A}(\bar{\nu},T)$, $\Delta\varepsilon^{A}(\bar{\nu},T)-\Delta\varepsilon(\bar{\nu},T_{iso})$, and the degree of anisotropy $R(\bar{\nu},T)$ has been proven to be an effect of the variation of order of the guest molecules in the liquid crystal phase and thus, can be taken for the determination of the CD and UV tensor coordinates.

For the evaluation of the $\Delta\varepsilon_{ii}^{*}$ $(i=1,2,3)$ *via* Eqs. (9) and (11) the elements of the order tensor g_{ii33}^{*} $(i=1,2,3)$ or the *Saupe* order parameters S^{*} and D^{*} have to be known as a function of temperature. Equation 9 depicts a plane in a $\Delta\varepsilon^{A}$, g_{2233}^{*}, g_{3333}^{*} space in which all measured points are on a curve which is determined by the typical dependence of S^{*} as a function of D^{*}. Fitting $\Delta\varepsilon^{A}(g_{2233}^{*},g_{3333}^{*})$ by taking into account the function $S^{*}(D^{*})$ with its corresponding experimentally obtained parameter δ yields three parameters which describe the plane (Fig. 21) from which the $\Delta\varepsilon_{ii}^{*}$ can be calculated [33]. The procedure can be either performed by taking Eq. (7) as an additional condition or not. In the later case, Eq. (7) can be taken for an independent check of the result of the fitting procedure. Both results are equal within the experimental error. There are two further assumptions: 1) One conformer or a temperature independent equilibrium of conformers exists. 2) The orientation of the principal axes of the order tensor with respect to the molecular frame is temperature independent. This very hidden assumption has been experimentally proven for the binaphthols to be acceptable [27] in spite of the fact that a small temperature dependence has been observed.

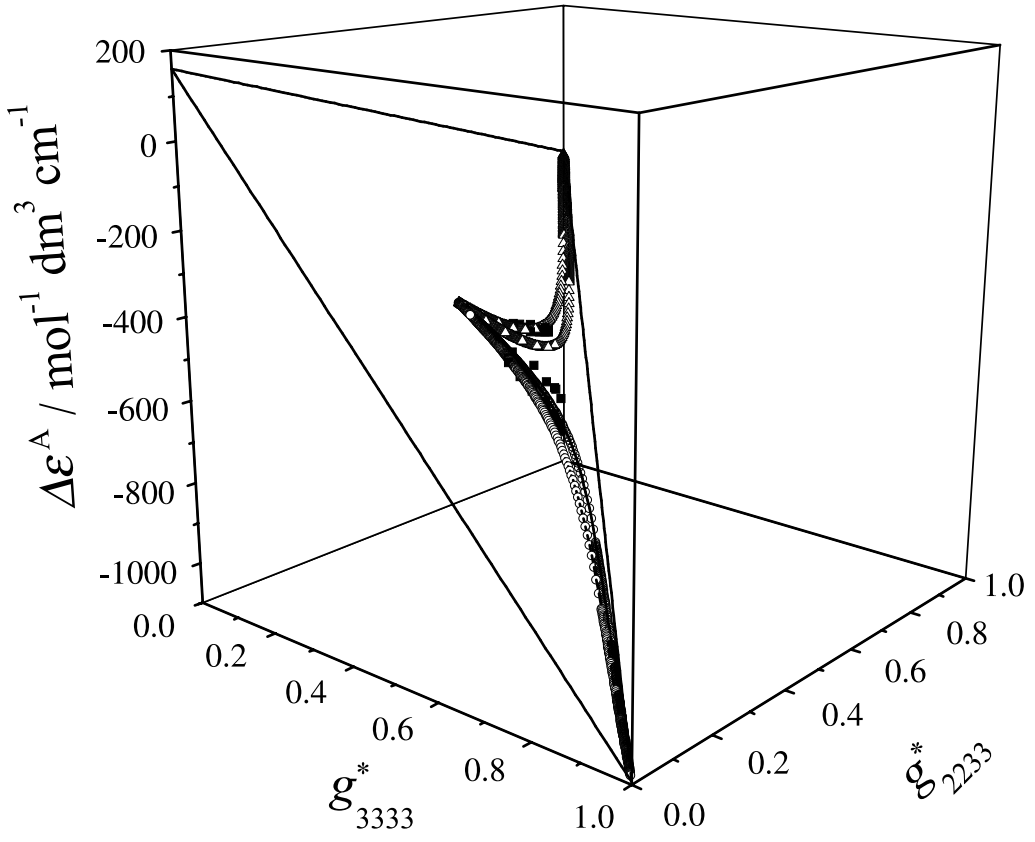

Fig. 21. The result of the fit (Eq. (9)) of the $\Delta\varepsilon^{A}$ as a function of the coordinates of the order tensor g_{2233} and g_{3333} for (*R*)-**9** and (*R*)-**10** with respect to the principal axes of the order tensor of (*R*)-**9** for the wavenumber of the negative maximum of the A→B transition $\bar{\nu}=43197\,\mathrm{cm}^{-1}$ (231.5 nm); $\Delta\varepsilon^{A}$ (■) and $\Delta\varepsilon_{calc}^{A}=A_j+B_j\,g_{3333}^{*}+C_j\,g_{2233}^{*}$ for $\delta=1.00$ ((○) and (△); right) and $\delta=0.85$ ((○) and (△); left); δ is a parameter which correlates the diagonal elements of the order tensor in the order triangle [35]

The small difference $\Delta\varepsilon^{A}(\bar{\nu}, T) - \Delta\varepsilon(\bar{\nu}, T_{iso})$ and the relatively large errors of the g^{*}_{ii33} values complicate a reliable determination of the $\Delta\varepsilon^{*}_{ii}$ values. In order to improve the results for (*R*)-**9** and (*R*)-**10**, which possess within the experimental errors equal CD and UV spectra, the tensor coordinates $\Delta\varepsilon^{*}_{ii}$ were determined in one and the same fitting procedure assuming equal $\Delta\varepsilon^{*}_{ii}$ for both compounds. Because the orientation axis of both molecules are differently oriented with respect to their molecular frame, the area of fitted values in the $\Delta\varepsilon^{A}$, g^{*}_{2233}, g^{*}_{3333} space is enlarged (Fig. 21). For (*R*)-**8** and the unbridged binaphthols a further approximation, derived from the results of (*R*)-**9** and (*R*)-**10**, namely that the product of $\Delta\varepsilon^{*}_{22}(g^{*}_{2233} - g^{*}_{1133})$ is negligible small in Eq. (9), has been used. In these cases only one tensor coordinate and the sum of two tensor coordinates can be evaluated.

Appendix

A.1. Calculation of the CD and UV Bands of an Exciton Band System (Fig. 1)

A negative couplet, *e.g.*, for a conformer of an unbridged 1,1′-binaphthol with a naphthyl–naphthyl dihedral angle ω between 0° and −90° to −110° (Fig. 2), results according to Eq. (2) from a negative and positive CD of the α (A→B) and β (A→A) transition, which are polarized perpendicularly (A→B) and parallelly (A→A) to the C_2 symmetry axis. The degree of anisotropy is calculated under the assumption that the orientation axis is oriented parallel to the C_2 symmetry axis of the molecule. The β (A→A) band is located at higher wavenumbers. Because the band shape of the CD and the absorption bands belonging to the α (A→B) and β (A→A) transitions has been assumed to be not symmetric the negative and positive peak of the calculated couplet are different in their heights.

A.2. Coordinates and Tensorial Description

In a description of the absorption process, the degree of anisotropy, the CD, and also the ACD nine quantities $X_{ij} = X_{ji}$ ($i, j = 1, 2, 3$) are needed. These quantities X_{11}, X_{12}, X_{13}, X_{21}, X_{22}, X_{23}, X_{31}, X_{32}, X_{33} are called the ''coordinates of the tensor $\underline{\underline{X}}$''. Instead of nine X_{ij}, only three diagonal elements X_{ii} and three *Eulerian* angles are sufficient to describe the molecular properties. The *Eularian* angles then describe the orientation of the principal axes of the tensor $\underline{\underline{X}}$, in which all $X_{ij} = 0$ for $i \neq j$, with respect to an arbitrary coordinate system chosen within the molecular skeleton. Five tensors are of exceptional importance for the ACD spectroscopy: the transition moment or the absorption tensor (D^{NK}_{ij} or ε_{ij}), the tensor of rotation or the circular dichroism tensor (R^{NK}_{ij} or $\Delta\varepsilon_{ij}$), and the order tensor (g_{ij33}). For molecules without symmetry the principal axes of these three different groups of tensors do not coincide and, therefore, one has to introduce three different coordinate systems in order to handle these phenomena: x^{+}_{i} for D^{NK}_{ij} or ε_{ij}, x°_{i} for R^{NK}_{ij} or $\Delta\varepsilon_{ij}$, and x^{*}_{i} for g_{ij33}.

A.3. Orientational Distribution Coefficients – Coordinates of the Order Tensor

The coordinates of the order tensors, needed to describe the long-range orientational order of molecules in a macroscopic phase, are defined by the orientational

distribution coefficients given by Eq. (A-1) where $f(\alpha, \beta, \gamma)$ is the orientational distribution function with the *Eulerian* angles α, β, and γ. The a_{ij}s are the elements of the transformation matrix from the molecular fixed to the space fixed coordinate system [11]. The orientational distribution coefficients g_{ijkk} ($k = 1, 2, 3$) are order tensors. All quantities with a superscript "*" are given with respect to the principal axes of the order tensor (Eq. (A-2)).

$$g_{ijkl} = \frac{1}{8\pi^2} \iiint_{\alpha,\beta,\gamma} f(\alpha, \beta, \gamma) a_{ik} a_{jl} \sin\beta \, d\alpha \, d\beta \, d\gamma, \quad i, j, k, l = 1, 2, 3 \qquad \text{(A-1)}$$

$$0 \leq g^*_{ii33} \leq 1 \text{ for } i = 1, 2, \text{or } 3 \quad \text{and} \quad \sum_{i=1}^{3} g^*_{ii33} = 1 \qquad \text{(A-2)}$$

The principal axes of g_{ij33} are fixed by symmetry for molecules with a point symmetry group different from C_1, C_2, C_i, C_s, and C_{2h} [34]. For C_2, C_s, and C_{2h} the orientation of two axes and for C_1 and C_i of all three axes with respect to the molecular skeleton have to be determined experimentally (by the measurement of all elements of g_{ij33}); the orientations of the x_i^* axes vary, in general, with temperature. The order triangle (Fig. 22) describes the area of numerical range of order parameters [34], the knowledge of which is often very important for an experimental analysis and the description of thermodynamic properties.

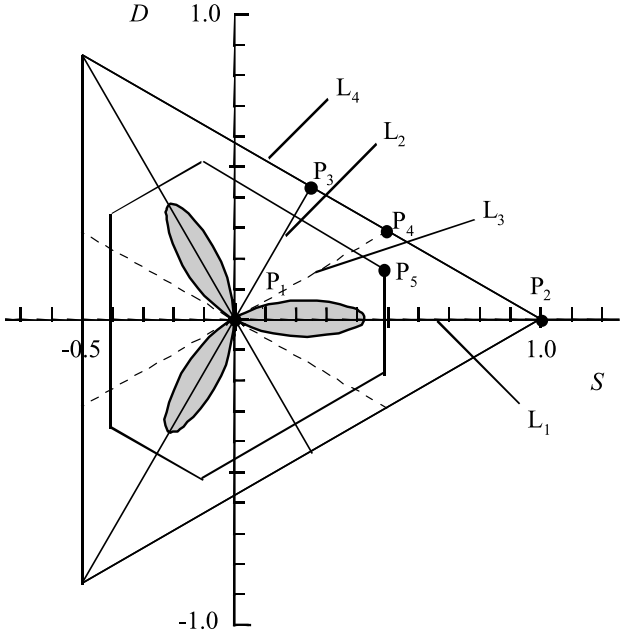

Fig. 22. The order triangle [12] is a graphical representation of all possible values of the order parameters S and D; the lines L_1 to L_4 are characteristic for special situations of the order: L_1: $g^*_{1133} = g^*_{2233}$, L_2: $g^*_{3333} = g^*_{2233}$, L_3: $g^*_{2233} = 1/3$, L_4: $g^*_{1133} = 0$; the points P_i (S^*, D^*) for $i = 1$ to 4 are outstanding points for the long-range orientational order: P_1 (0, 0), P_2 (1, 0), P_3 $(1/4, \sqrt{3}/4)$, P_4 $(1/2, \sqrt{3}/6)$, $P_5 = P(S^*, D^*)$; the three shaded lobes are the area of order parameter which can not exist in a stable liquid crystal phase; only the order parameters (S^*, D^*), *i.e.* P_5, characterize the order in a way which is suitable to compare the order of different compounds

A.4. Operators and Matrix Elements (Eq. (A-3))

$$\mu_i = -\mathrm{e}\sum_{\nu} x_{i\nu}; \quad \langle p_k\rangle_{nm} = -\mathrm{im}\omega_{nm}\langle x_k\rangle_{nm};$$

$$m_r = \frac{1}{2}\sum_{i,j}\varepsilon_{ijr}m_{ij} = -\frac{\mathrm{e}}{2\mathrm{mc}}\sum_{i,j}\sum_{\nu}\varepsilon_{rij}x_{i\nu}p_{j\nu}; \quad \mathrm{Q}_{ij} = -\frac{\mathrm{e}}{2}\sum_{\nu}x_{i\nu}x_{j\nu}. \tag{A-3}$$

ν is the index for the sum over all electrons. Matrix elements often used for the theoretical description are (Eqs. (A-4)–(A-6)).

$$\langle\mu_i\rangle_{0\mathrm{n}} = \langle\Psi_0|\mu_i|\Psi_\mathrm{n}\rangle; \quad \langle m_i\rangle_{\mathrm{n}0} = \langle\Psi_\mathrm{n}|m_i|\Psi_0\rangle; \quad \langle Q_{ij}\rangle_{0\mathrm{n}} = \langle\Psi_0|Q_{ij}|\Psi_\mathrm{n}\rangle;$$

$$\langle m_{ij}\rangle_{\mathrm{n}0} = -\frac{\mathrm{e}}{2\mathrm{mc}}\left\langle\sum_{\nu}\left(x_{i\nu}p_{j\nu} - x_{j\nu}p_{i\nu}\right)\right\rangle; \quad \langle m_r\rangle_{\mathrm{n}0} = \frac{1}{2}\sum_{i,j}\varepsilon_{ijr}\langle m_{ij}\rangle_{\mathrm{n}0}; \tag{A-4}$$

$$\langle Q_{ij}\rangle_{\mathrm{n}0} = -\frac{\mathrm{e}}{2}\left\langle\sum_{\nu}x_{i\nu}x_{j\nu}\right\rangle_{\mathrm{n}0} \tag{A-5}$$

$$\langle C_{sj}\rangle_{\mathrm{n}0} = -\mathrm{i}\varepsilon_{sjr}\langle m_r\rangle_{\mathrm{n}0} - \frac{\omega_{\mathrm{n}0}}{\mathrm{c}}\langle Q_{sj}\rangle_{\mathrm{n}0}; \quad \langle C_{ij}\rangle_{\mathrm{n}0} = -\mathrm{i}\langle m_{ij}\rangle_{\mathrm{n}0} - \frac{\omega_{\mathrm{n}0}}{\mathrm{c}}\langle Q_{ij}\rangle_{\mathrm{n}0} \tag{A-6}$$

A.5. CD and UV Tensor Coordinates

The CD tensor coordinates of a chirality measurement, *i.e.*, $\Delta\varepsilon^*_{11}$, $\Delta\varepsilon^*_{22}$, and $\Delta\varepsilon^*_{33}$, need a simple interpretation because it is not possible to measure them directly in one and the same experiment. They are the results of circular dichroism measurements with light beams propagating along the x^*_1, x^*_2, and x^*_3 directions, respectively, when the ensemble of molecules are rotationally symmetrically distributed about the propagation direction of the measuring light beam: about x^*_1 for $\Delta\varepsilon^*_{11}$, about x^*_2 for $\Delta\varepsilon^*_{22}$, and about x^*_3 for $\Delta\varepsilon^*_{33}$. The transition moment tensor is a general vector product $\varepsilon_{ij} = \langle\mu_i\rangle\langle\mu_j\rangle$ and, thus can be traced back to the transition moment vector ($\langle\mu_i\rangle$ and $\langle\mu_j\rangle$ are the coordinates – components – of the vector with respect to a chosen coordinate system). The direction of the transition moment vector describes the direction within the molecule in which the light must be polarized in order to have its maximal absorption. The scalar product of the transition moment vector$\langle\vec{\mu}\rangle^2$ is proportional to the absorption coefficient.

A CD tensor coordinate can be decomposed into an electric dipole/magnetic dipole and in an electric dipole/electric quadrupole contribution. The latter do not contribute to the CD of isotropic phases (Eqs. (A-7)–(A-9)).

$$\Delta\varepsilon_{ij} = \Delta\varepsilon^{\mu m}_{ij} + \Delta\varepsilon^{\mu\mathrm{Q}}_{ij} \tag{A-7}$$

$$\Delta\varepsilon^{\mu m}_{11}(\bar{\nu}) = -\frac{\mathrm{i}}{2}B\bar{\nu}\sum_{n}\left(\langle\mu_2\rangle_{0\mathrm{n}}\langle m_2\rangle_{\mathrm{n}0} + \langle\mu_3\rangle_{0\mathrm{n}}\langle m_3\rangle_{\mathrm{n}0}\right)G^{0\mathrm{n}}(\bar{\nu}) \tag{A-8}$$

$$\Delta\varepsilon^{\mu\mathrm{Q}}_{11}(\bar{\nu}) = \frac{1}{2}B\bar{\nu}\sum_{n}\frac{\omega_{\mathrm{no}}}{\mathrm{c}}\left(-\langle\mu_2\rangle_{0\mathrm{n}}\langle Q_{31}\rangle_{\mathrm{n}0} + \langle\mu_3\rangle_{0\mathrm{n}}\langle Q_{21}\rangle_{\mathrm{n}0}\right)G^{0\mathrm{n}}(\bar{\nu}) \tag{A-9}$$

$\Delta\varepsilon^{\mu m}_{22}(\bar{\nu})$ and $\Delta\varepsilon^{\mu m}_{33}(\bar{\nu})$ can be obtained by cyclic permutation of the indices of $\Delta\varepsilon^{\mu m}_{11}(\bar{\nu})$ (Eq. (A-8)) whereas $\Delta\varepsilon^{\mu\mathrm{Q}}_{22}(\bar{\nu})$ and $\Delta\varepsilon^{\mu\mathrm{Q}}_{33}(\bar{\nu})$ are analogously obtained from Eq. (A-9).

It has to be mentioned here that the evaluated $\Delta\varepsilon_{ij}^{\mu Q}$ are, except some special situations, origin dependent, in general. If they are origin independent then these electric dipole/electric quadrupole terms can be determined experimentally from $\Delta\varepsilon_{ii}^{*}$. The integration over the Δ_i^{*} yields the corresponding matrix elements for the contribution of single transitions to the ACD (Eqs. (A-11)–(A-13)).

$$\frac{1}{2}\left(R_{11}^{n0} - R_{22}^{n0} - R_{33}^{n0}\right) = \frac{i}{2}\langle\mu_1\rangle_{0n}\langle m_1\rangle_{n0} + R_{11}^{\mu Q} \qquad \text{(A-11)}$$

$$\frac{1}{2}\left(R_{22}^{n0} - R_{11}^{n0} - R_{33}^{n0}\right) = \frac{i}{2}\langle\mu_2\rangle_{0n}\langle m_2\rangle_{n0} + R_{22}^{\mu Q} \qquad \text{(A-12)}$$

$$\frac{1}{2}\left(R_{33}^{n0} - R_{11}^{n0} - R_{22}^{n0}\right) = \frac{i}{2}\langle\mu_3\rangle_{0n}\langle m_3\rangle_{n0} + R_{33}^{\mu Q} \qquad \text{(A-13)}$$

Acknowledgements

Financial support from the "Deutsche Forschungsgemeinschaft" and the "Fonds der Chemischen Industrie" is gratefully acknowledged.

References

[1] Berova N, Nakanishi K, Woody RW (eds) (2000) Circular dichroism. Principles and applications for biologists. Wiley, New York
[2] Lightner DA, Gurst JE (2000) Organic Conformational Analysis and Stereochemistry from Circular Dichroism Spectroscopy. Wiley-VCH, New York
[3] Kuball HG (2005) Chiroptical Analysis. In: Worsfold PJ, Townshend A, Poole CF (eds) Encyclopedia of Analytical Science, 2nd ed, vol 1. Elsevier, Oxford, p 60
[4] Diedrich C, Grimme S (2003) J Phys Chem **A107**: 2524
[5] Mason SF, Seal RH, Roberts RD (1974) Tetrahedron **30**: 1671
[6] Harada N, Nakanishi K (1969) J Am Chem Soc **91**: 3989
[7] Nakanishi K, Harada N (1983) Circular Dichroic Spectroscopy – Exciton Coupling in Organic Stereochemistry. University Science Books, University Science Books, Mill Valley
[8] Michl J, Thulstrup EW (1986) Spectroscopy with polarized light – Solute Alignment by Photoselection, in Liquid Crystal, Polymers, and Membranes. VCH, New York
[9] Kuball HG, Friesenhan H, Schönhofer A (1988) Optical Activity of Oriented Molecules. In: Samori B, Thulstrup EW (eds) Polarized Spectroscopy of Ordered Systems, NATO ASI Series. Series C: Mathematical and Physical Sciences, vol 242. Kluwer, Dordrecht, p 391
[10] Kuball HG (2002) Enantiomer **7**: 197
[11] Kuball HG, Karstens T, Schönhofer A (1976) Chem Phys **12**: 1
[12] Kuball HG, Strauss A, Kappus M, Fechter-Rink E, Schönhofer A, Scherowsky G (1987) Ber Bunsenges Phys Chem **91**: 1266
[13] Asahi T, Kobayashi J (2003) Polarimeter for Optically Active Materials. In: Weiglhofer WS, Lakhtakia A (eds) Introduction to Complex Mediums for Optics and Electromagnetics. Spie Press, Bellingham WA, USA, p 645
[14] Kuball HG, Sieber G, Neubrech S, Schultheis B (1993) Chem Phys **169**: 335
[15] Hansen AE, Bak KL (1999) Enantiomer **4**: 455
[16] Hansen AE, Bak KL (2000) J Phys Chem **A104**: 11362
[17] Hansen AE (2005) this volume
[18] Heppke G, Lötzsch D, Oestreicher F (1987) Z Naturforsch **42a**: 279; We are grateful to Prof. Dr. *G. Heppke* and Dr. *F. Oestreicher*, TU Berlin, for supplying us with the compound (*S*)-**1**

[19] Merck Kga A, Darmstadt
[20] Bonnett R, Davies JE, Hursthouse MB, Sheldrick GM (1978) Proc R Soc London Ser B **202**: 249
[21] Moscowitz A, Wellmann KM, Djerassi C (1963) J Am Chem Soc **85**: 3515
[22] Killet CL (1995) PhD Thesis. University Kaiserslautern (to be published)
[23] Nakanishi K, Berova N (1991) Lecture and Posters, 4th International Conference on CD, Bochum
[24] Weiss B (1999) PhD Thesis. University Kaiserslautern (to be published)
[25] Beck AK, Dobler DA, Plattner DA (1997) Helv Chim Acta **80**: 2073
[26] Dorr E (1999) PhD Thesis. University Kaiserslautern (to be published)
[27] Kiesewalter I (1999) PhD Thesis. University Kaiserslautern (to be published)
[28] Canonica S, Wild UP (1991) J Phys Chem **95**: 6535
[29] Kuball HG, Türk O, Kiesewalter I, Dorr E (2000) Mol Cryst Liq Cryst **352**: 195
[30] Kuball HG, Höfer T (2001) From a Chiral Molecule to a Chiral Anisotropic Phase. In: Kitzerow HS, Bahr Ch (eds) Chirality in Liquid Crystals – Partially Ordered Systems. Springer, New York, p 67
[31] Snatzke G (1991) Helicity of Molecules, Different Definitions and Application to Circular Dichroism. In: Janoschek R (ed) Chirality – From Weak Bosons to the α-Helix, p 59
[32] Snir J, Schellman J (1973) J Phys Chem **77**: 1653
[33] Höfer T (2000) PhD Thesis. University Kaiserslautern (to be published)
[34] Kuball HG, Memmer R, Strauss A, Junge M, Scherowsky G, Schönhofer A (1989) Liq Cryst **5**: 969
[35] Luckhurst GR, Zannoni C, Nordio PL, Segre U (1975) Mol Phys **30**: 1345
[36] Mori K, Masuda Y, Kashino S (1993) Acta Cryst **C49**: 1225
[37] Gridunova GV, Shklover VE, Struchkov YT, Chayanov BA (1983) Krystallografiya 28
[38] Reiß G, Frank W, University of Düsseldorf (to be published). We are grateful to Prof. Dr. *W. Frank* and Dr. *G. J. Reiß*, University Düsseldorf, for the X-ray analysis of these compounds